

Examining the Robustness of a Theophylline Cocrystal during Grinding with Additives Heba Abourahma*^a, Jennifer M. Urban^a, Nicole Morozowich^b and Benny Chan^a

^a Department of Chemistry, The College of New Jersey, 2000 Pennington Rd, Ewing, NJ 08628, USA

^b Department of Chemistry, Penn State University, 104 Chemistry Building, University Park, PA 16802

Electronic Supplementary Information

Table of Contents

- S1- PXRD characterization data for experiments involving benzamide (BZA)
- S2- PXRD characterization data for experiments involving benzoic acid (BA)
- S3- PXRD characterization data for experiments involving *p*-nitrophenol (*p*NP)
- S4- PXRD characterization data for experiments involving hydroquinone (HDQ)
- S5- PXRD characterization data for experiments involving *m*-hydroxybenzoic acid (*m*HBA)
- S6- PXRD characterization data for experiments involving *p*-(*N,N*-dimethylamino)benzoic acid dMABA
- S7- PXRD characterization data for experiments involving *p*-nitrobenzoic acid (*p*NBA)
- S8- PXRD and DSC characterization data for experiments involving salicylic acid (SA)
- S9- PXRD characterization data for experiments involving melamine (MLM)
- S10- PXRD characterization data for experiments involving acetamide (ACA)
- S11- PXRD and DSC characterization data for experiments involving 3,5-dinitrobenzoic acid (dNBA)
- S12- PXRD patterns for dMABA before and after grinding
- S13- PXRD patterns for dNBA before and after grinding
- S14- PXRD patterns for *m*HBA before and after grinding
- S15- PXRD pattern of TP•ACA cocrystal obtained from solution
- S16- ¹H NMR spectrum of TP.ACA in DMSO-d₆
- S17. IR spectrum of TP•ACA cocrystal
- S18- PXRD pattern of TP•MLM•DMSO cocrystal crystallized from solution
- S19. ¹H NMR spectrum of TP•MLM•DMSO in DMSO-d₆
- S20. Crystal data and structure refinement for TP•MLM•DMSO
- S21. Table of hydrogen bonds for TP•MLM•DMSO
- S22. Crystal structure of TP•MLM•DMSO

S1- PXRD characterization data for experiments involving benzamide (BZA)

Fig. S1a- PXRD patterns for competition and selectivity experiments involving BZA.

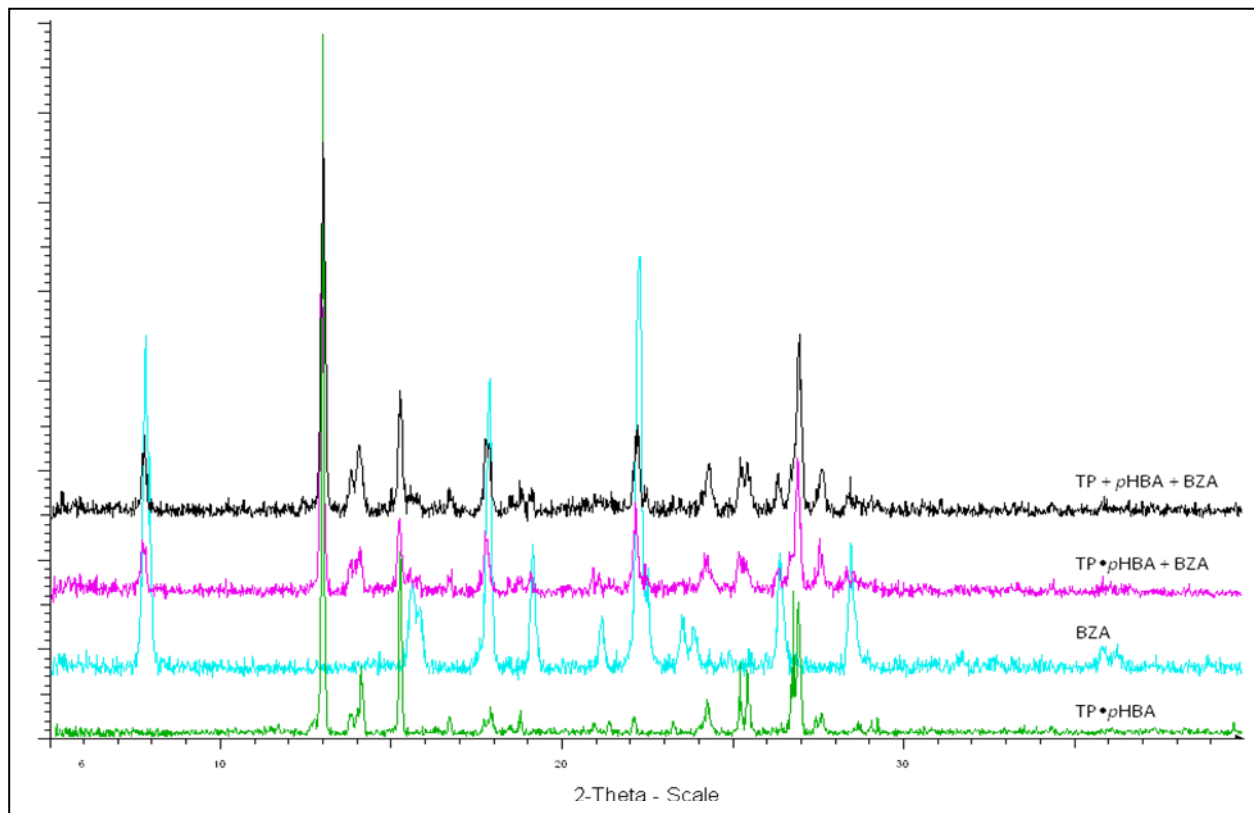
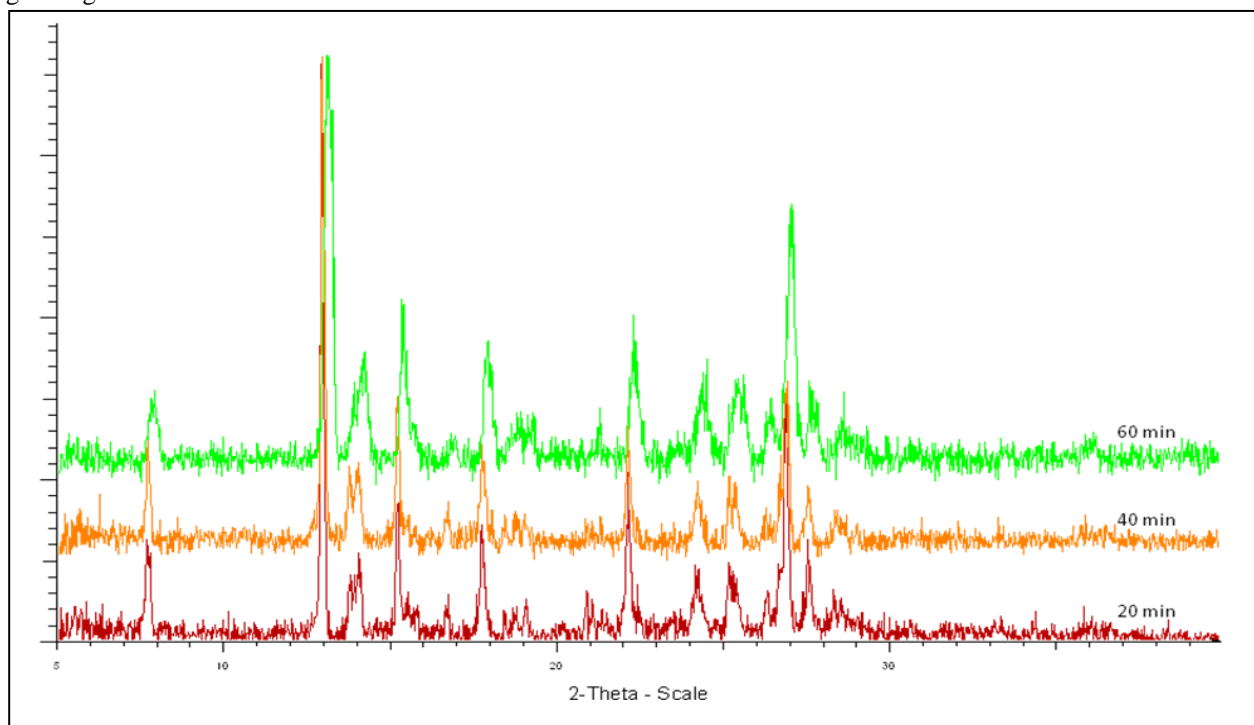


Fig.S1b- PXRD patterns for competition experiments involving TP•pHBA and BZA that examine the effect of grinding time on reaction outcome



S2- PXRD characterization data for experiments involving benzoic acid (BA)

Fig. S2a- PXRD patterns for competition and selectivity experiments involving BA.

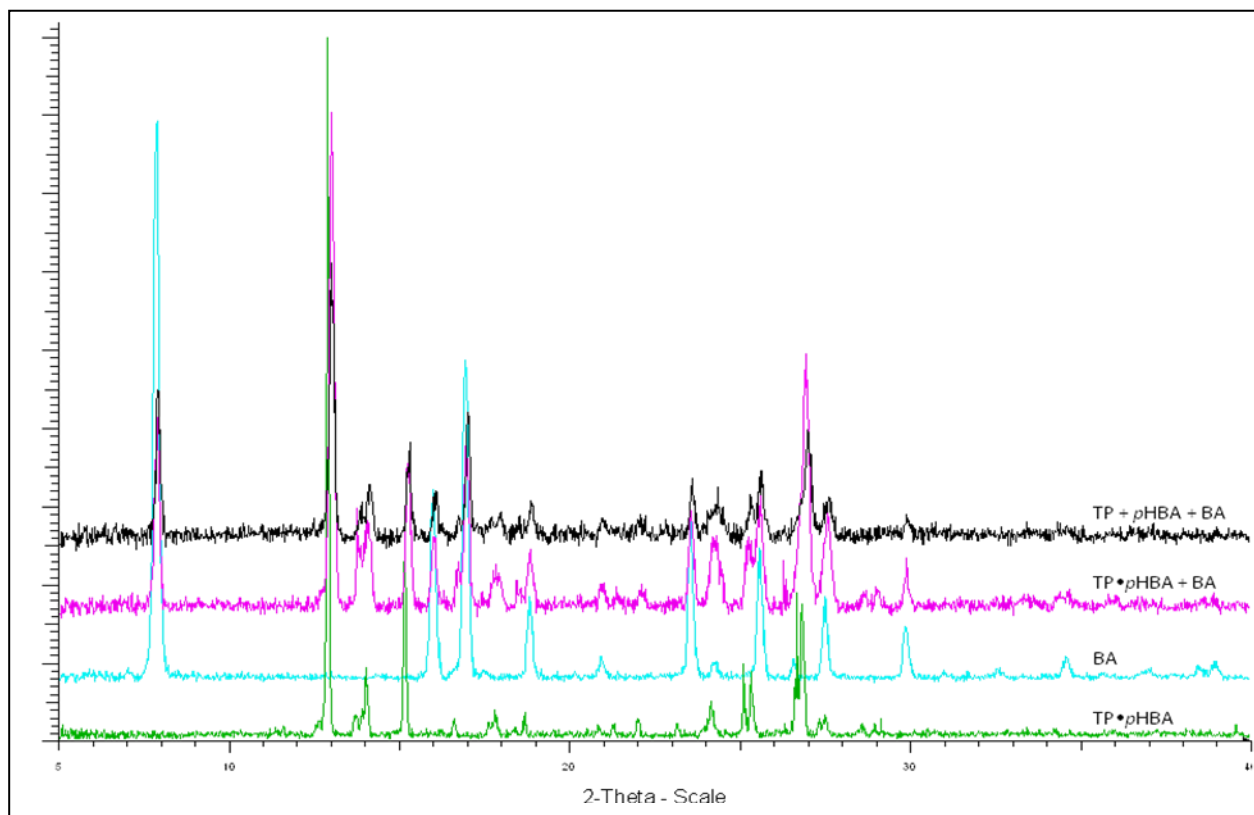
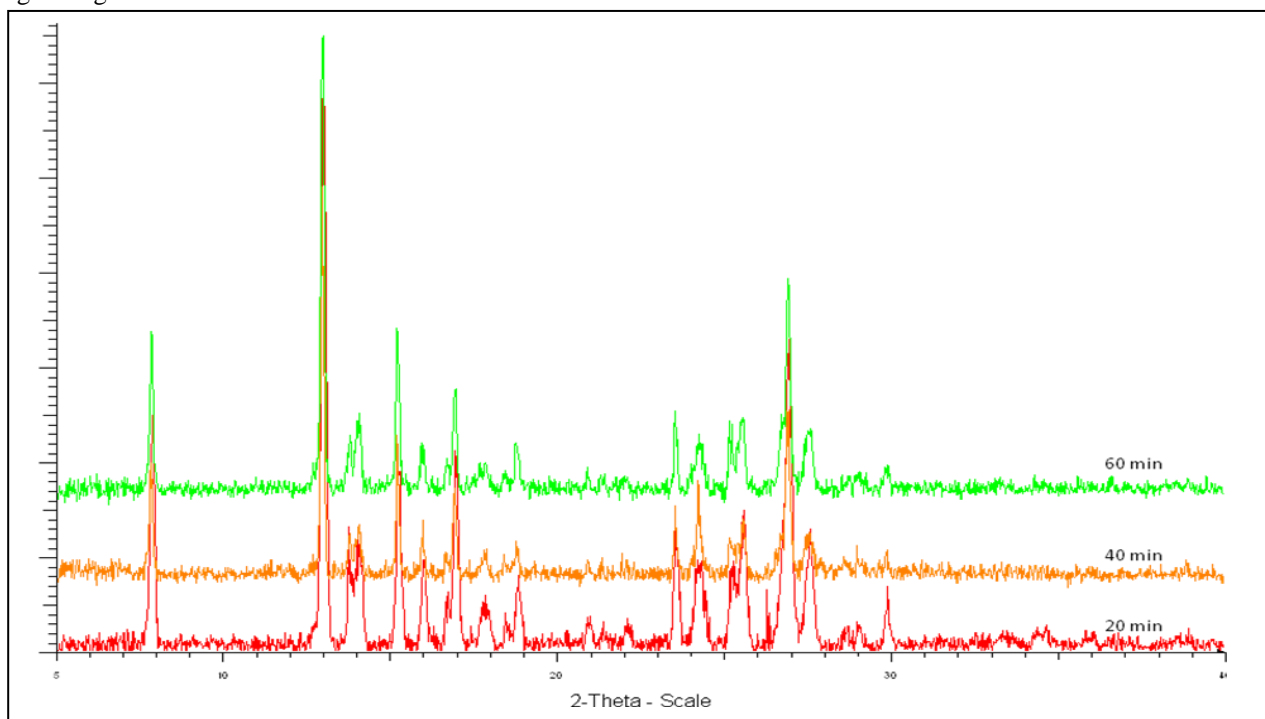


Fig.S2b- PXRD patterns for competition experiments involving TP•pHBA and BA that examine the effect of grinding time on reaction outcome



S3- PXRD characterization data for experiments involving *p*-nitrophenol (*p*NP)

Fig. S3a- PXRD patterns for competition and selectivity experiments involving *p*NP

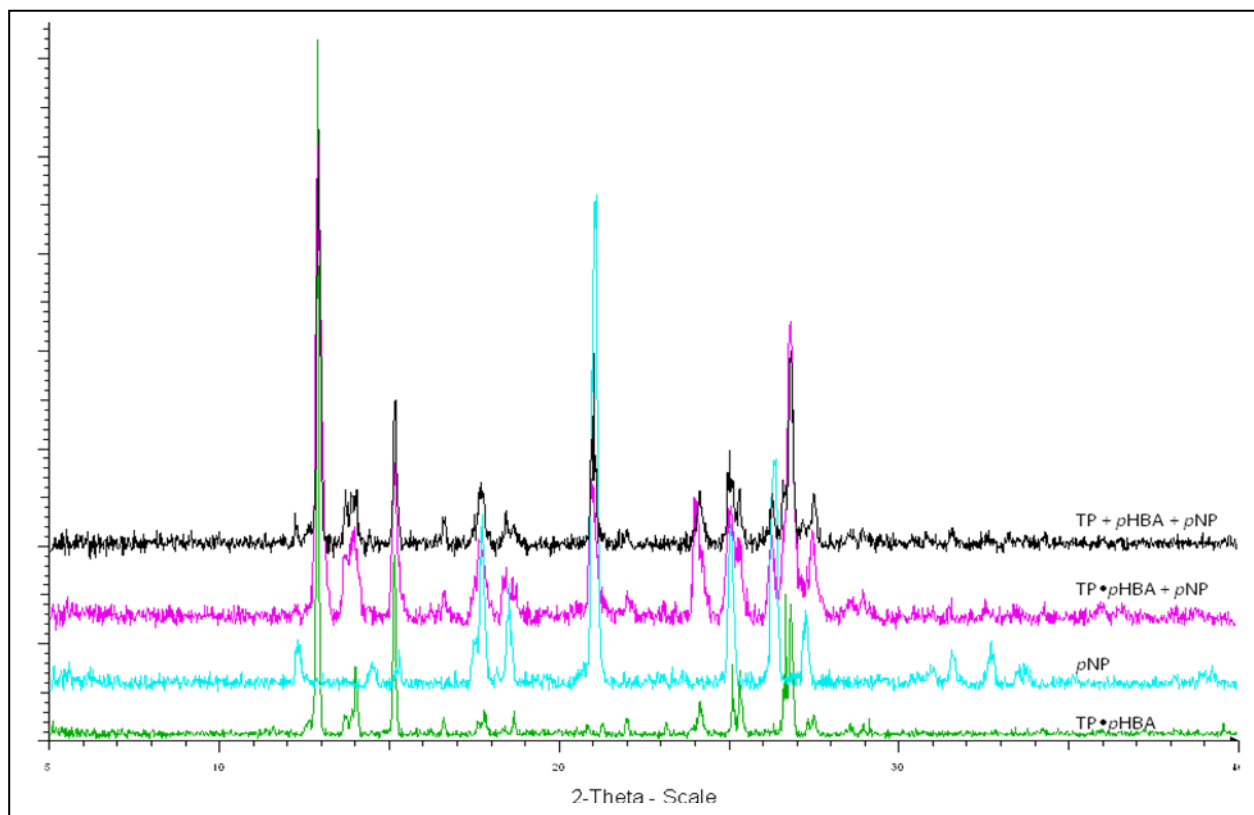
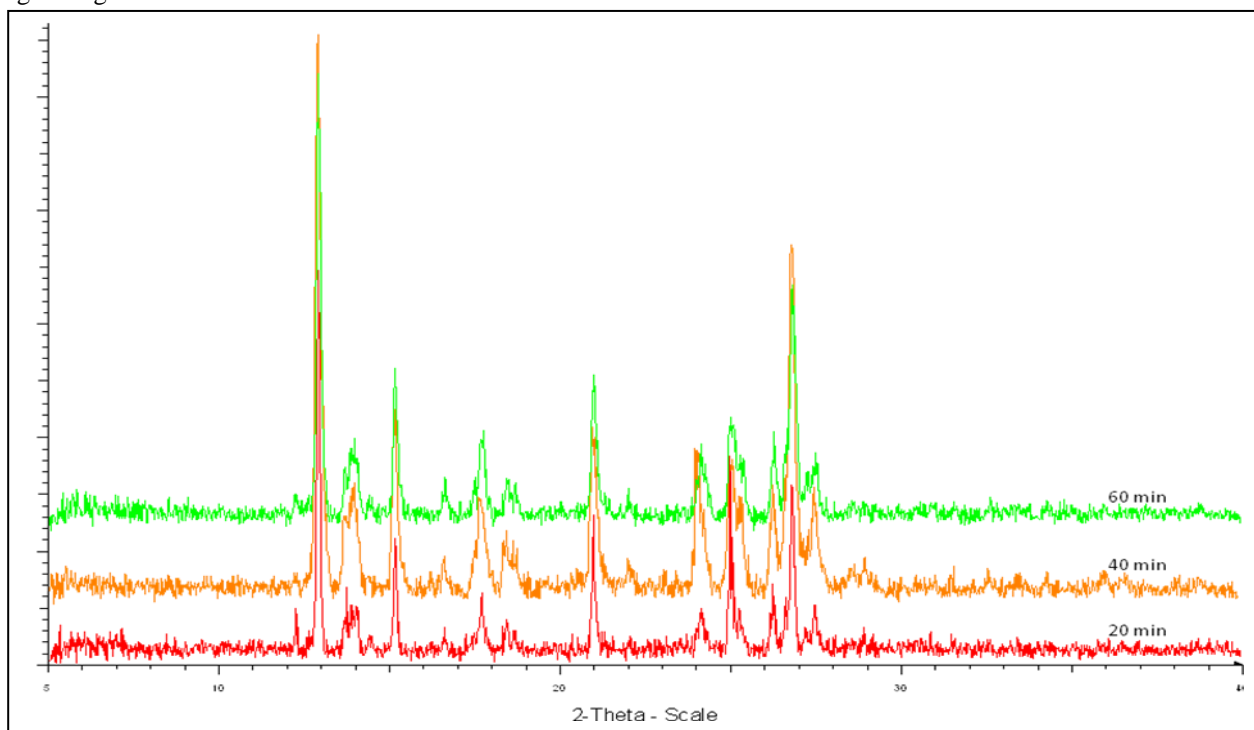


Fig.S3b- PXRD patterns for competition experiments involving TP•pHBA and *p*NP that examine the effect of grinding time on reaction outcome



S4- PXRD characterization data for experiments involving hydroquinone (HDQ)

Fig. S4a- PXRD patterns for competition and selectivity experiments involving HDQ.

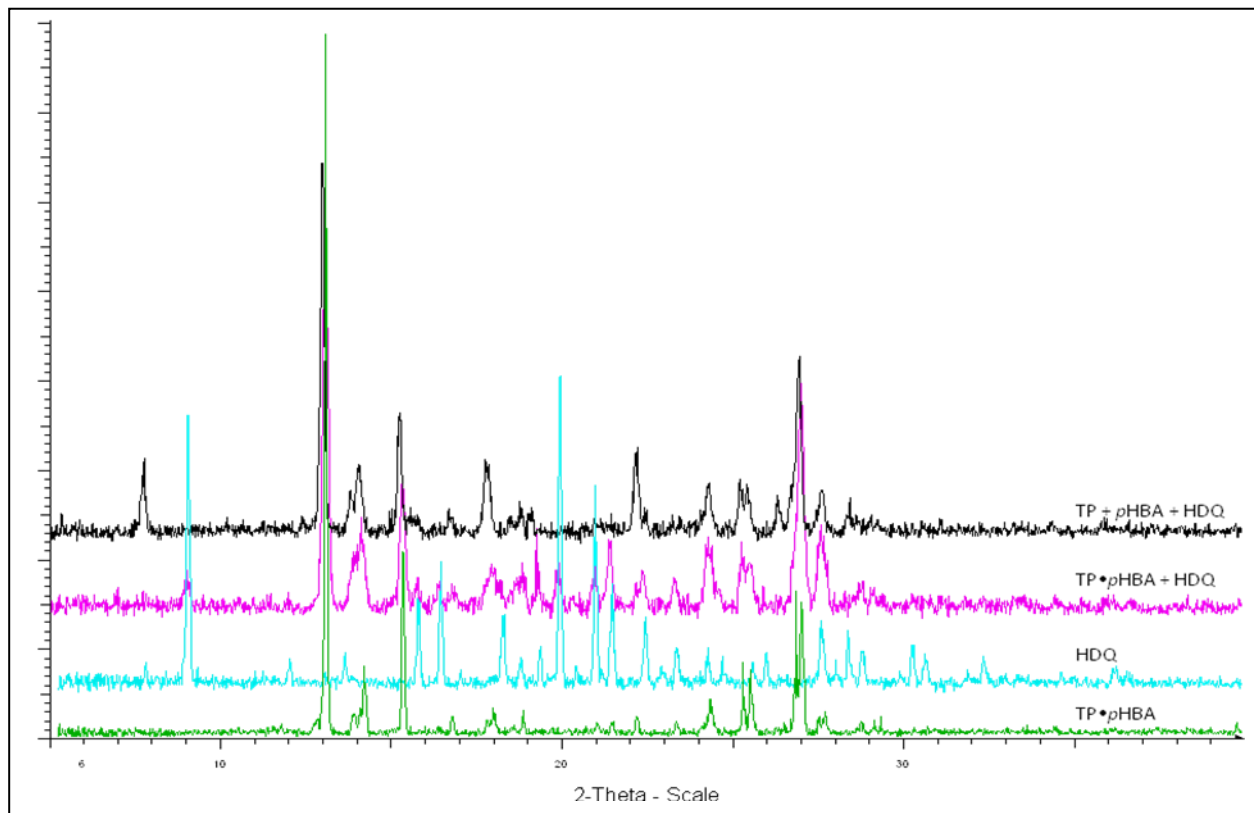
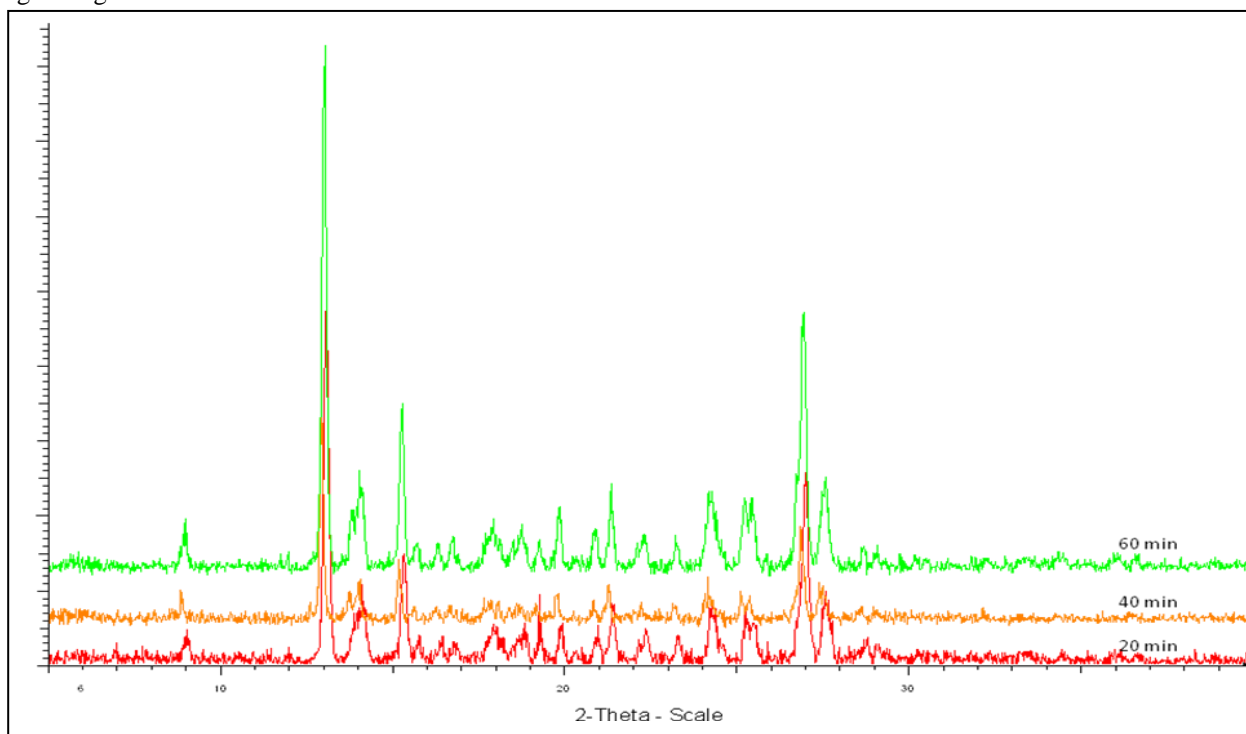


Fig.S4b- PXRD patterns for competition experiments involving TP•pHBA and HDQ that examine the effect of grinding time on reaction outcome



S5- PXRD characterization data for experiments involving *m*-hydroxybenzoic acid (*m*HBA)

Fig. S5a- PXRD patterns for competition and selectivity experiments involving *m*HBA.

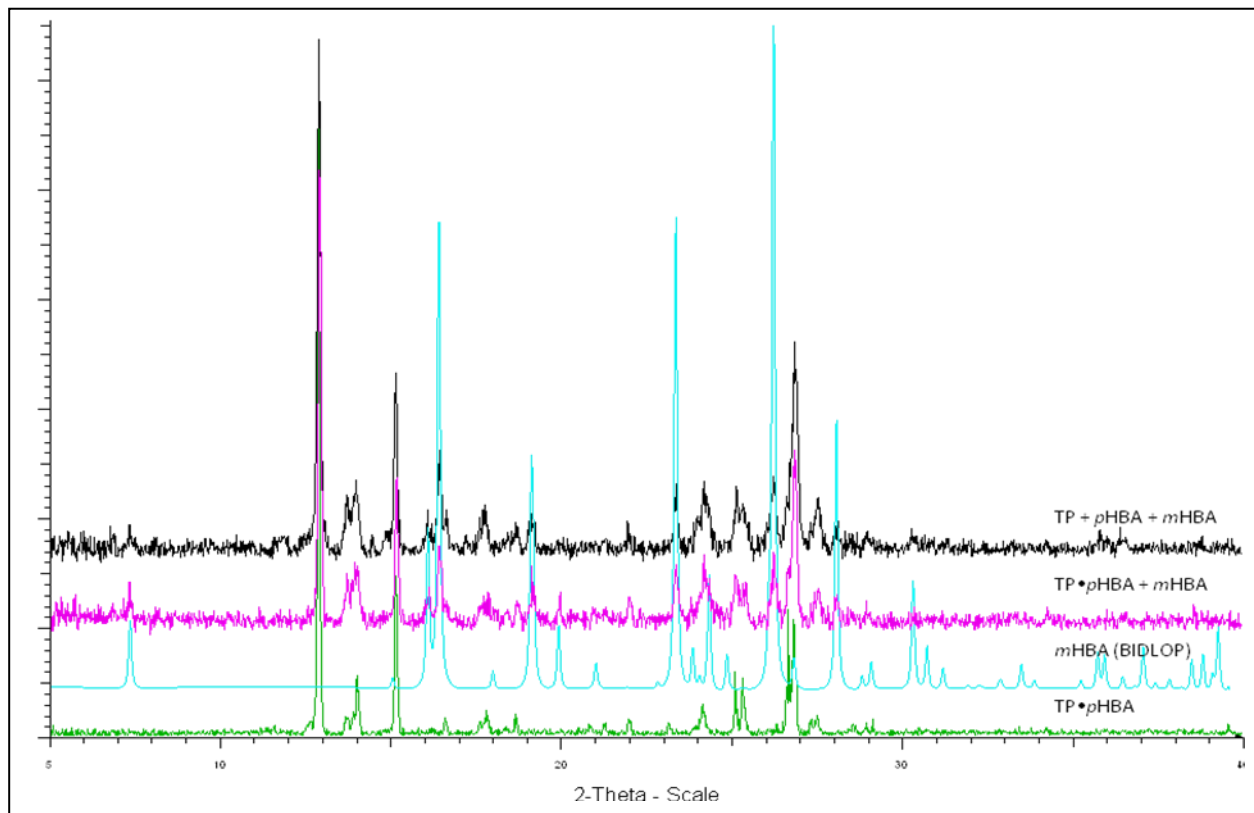
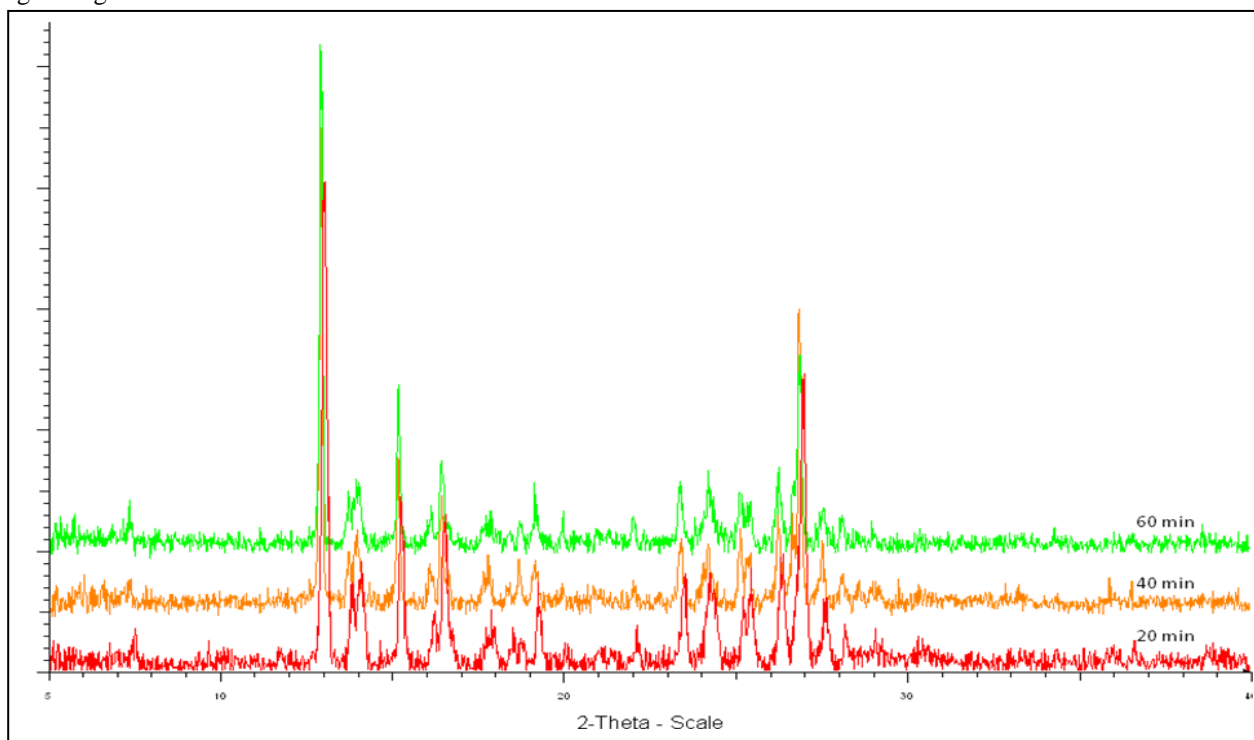


Fig.S5b- PXRD patterns for competition experiments involving TP • *p*HBA and *m*HBA that examine the effect of grinding time on reaction outcome



S6- PXRD characterization data for experiments involving *p*-(*N,N*-dimethylamino)benzoic acid (dMABA)

Fig. S6a- PXRD patterns for competition and selectivity experiments involving dMABA.

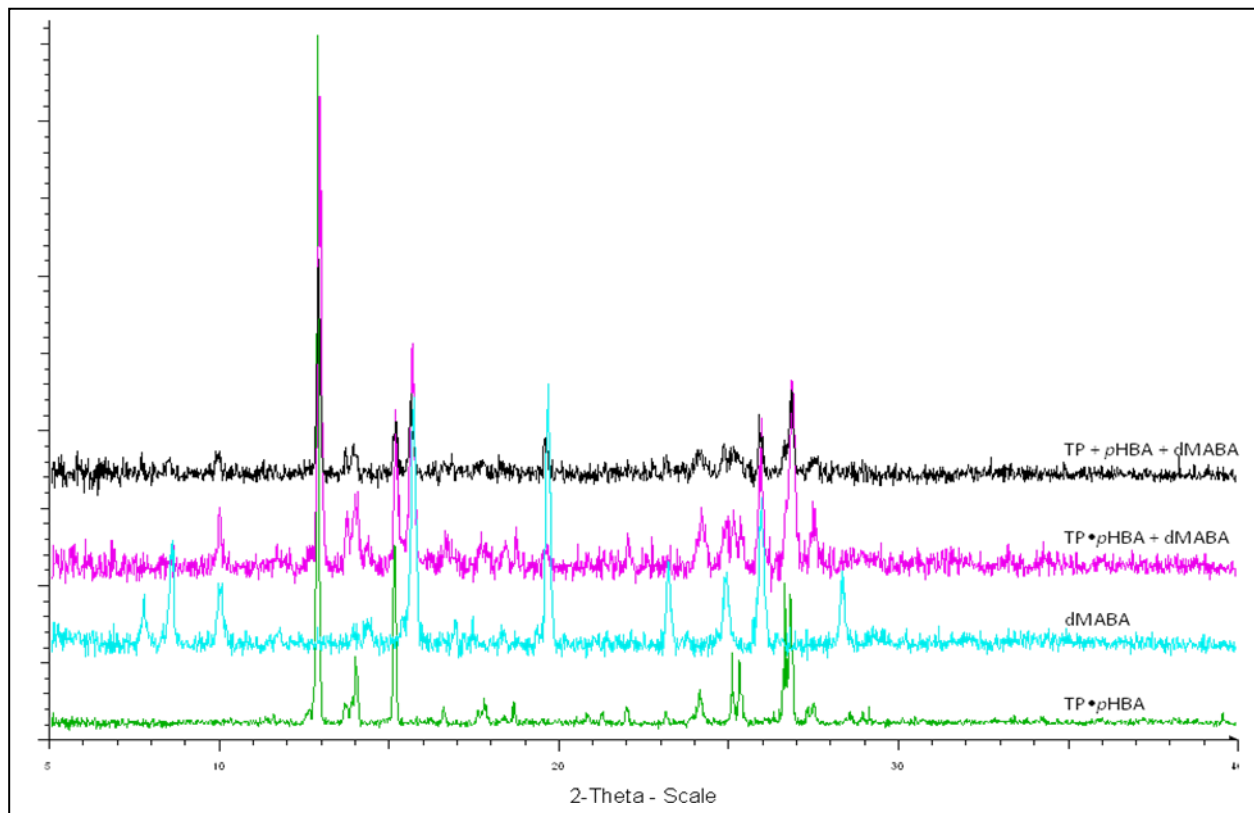
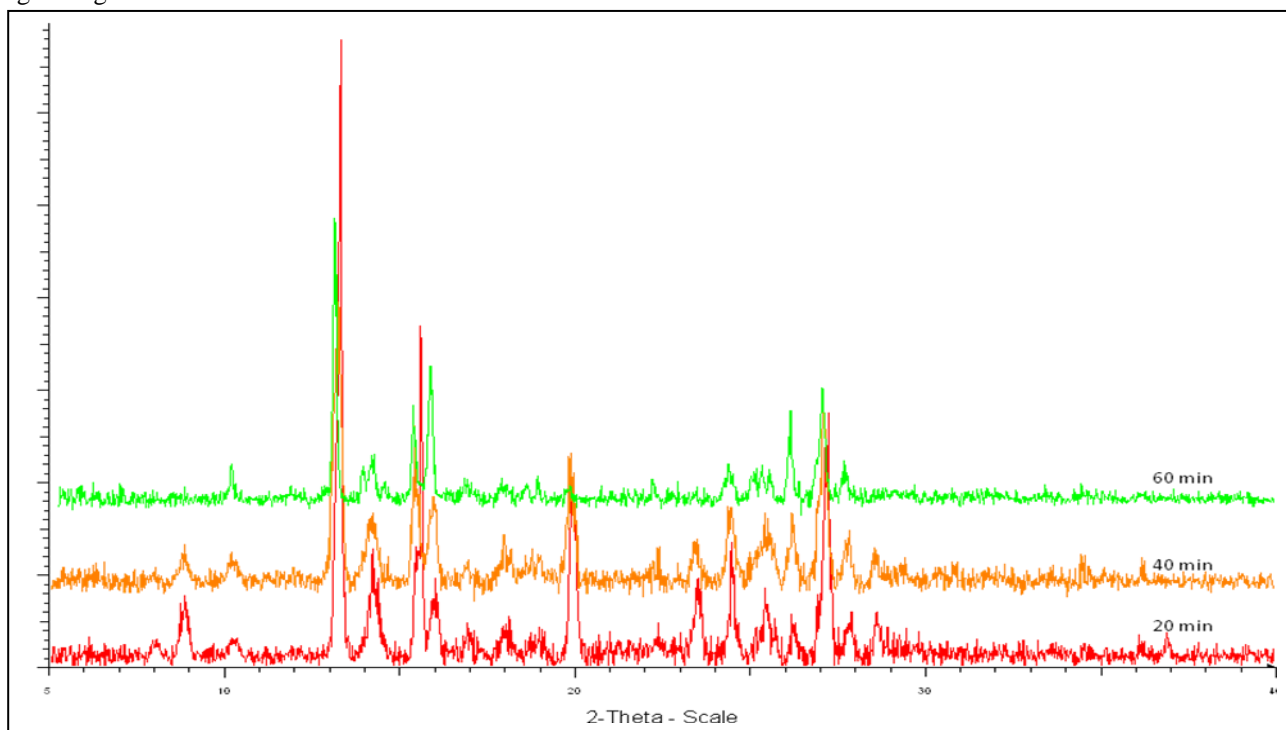
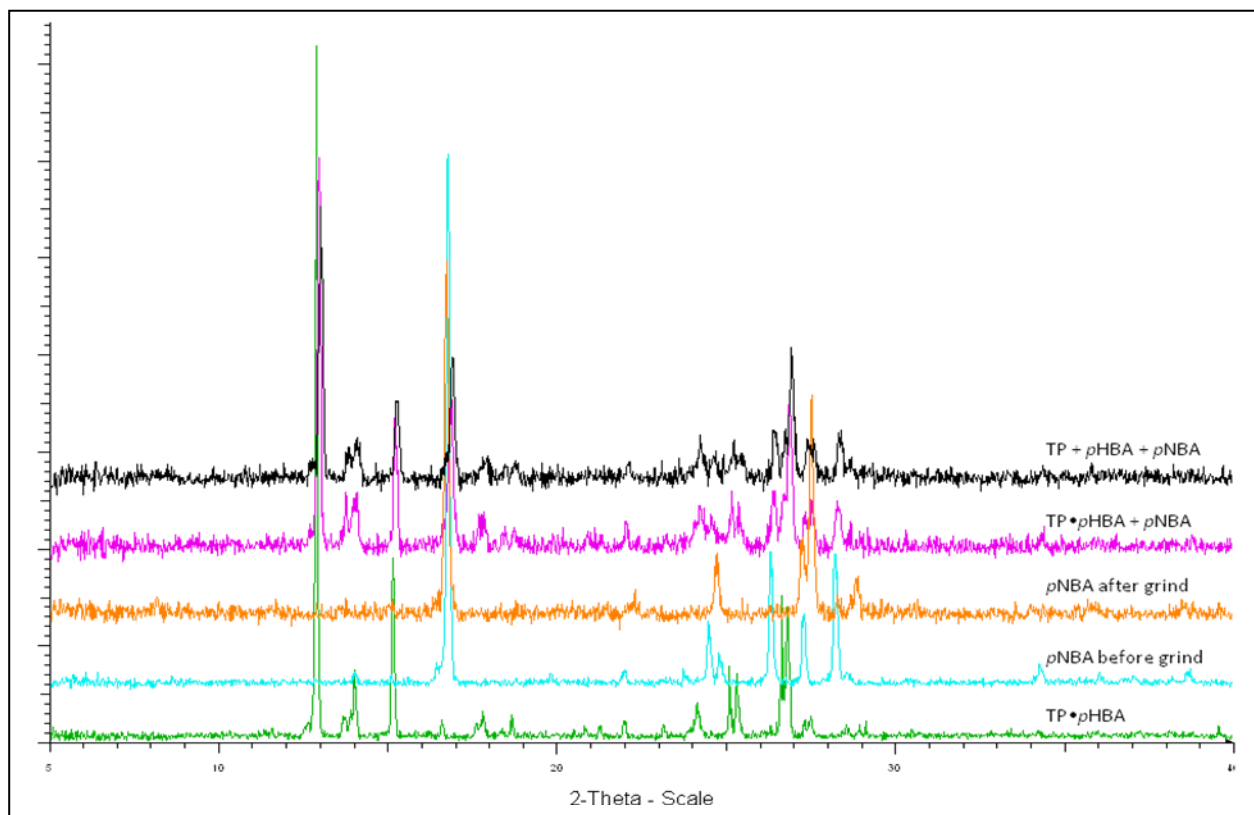


Fig.S6b- PXRD patterns for competition experiments involving TP•pHBA and dMABA that examine the effect of grinding time on reaction outcome



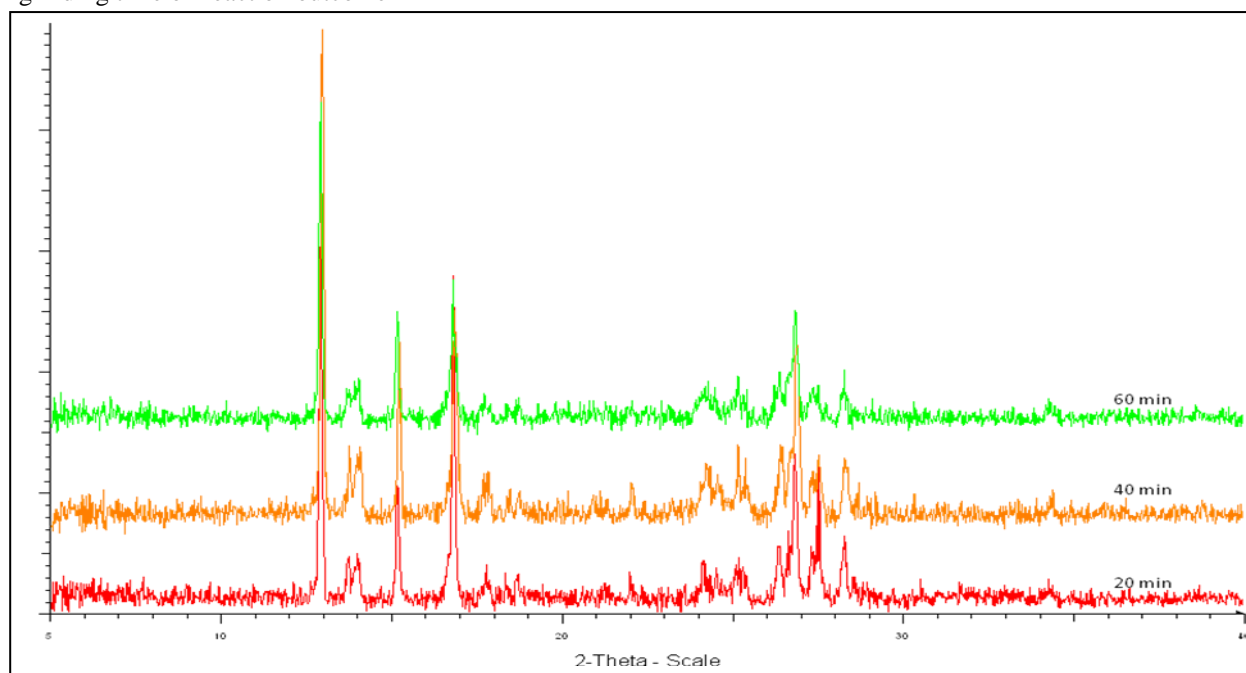
S7- PXRD characterization data for experiments involving *p*-nitrobenzoic acid (*p*NBA)

Fig. S7a- PXRD patterns for competition and selectivity experiments involving *p*NBA.



*Grinding commercial *p*NBA results in a mixture of two polymorphs,

Fig.S7b- PXRD patterns for competition experiments involving TP•*p*HBA and *p*NBA that examine the effect of grinding time on reaction outcome



S8- PXRD characterization data for experiments involving salicylic acid (SA)

Fig. S8a- PXRD patterns for competition and selectivity experiments involving SA.

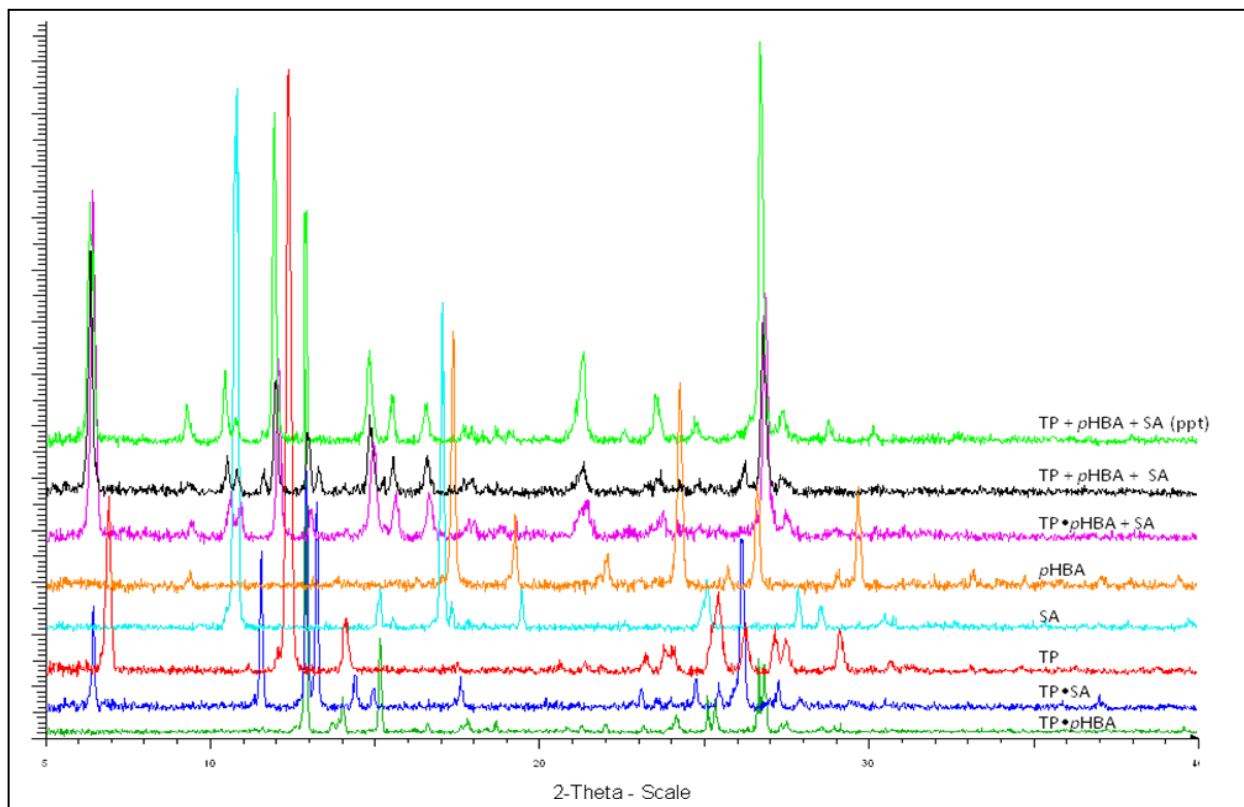


Fig.S8b- PXRD patterns for competition experiments involving TP•pHBA and SA that examine the effect of grinding time on reaction outcome

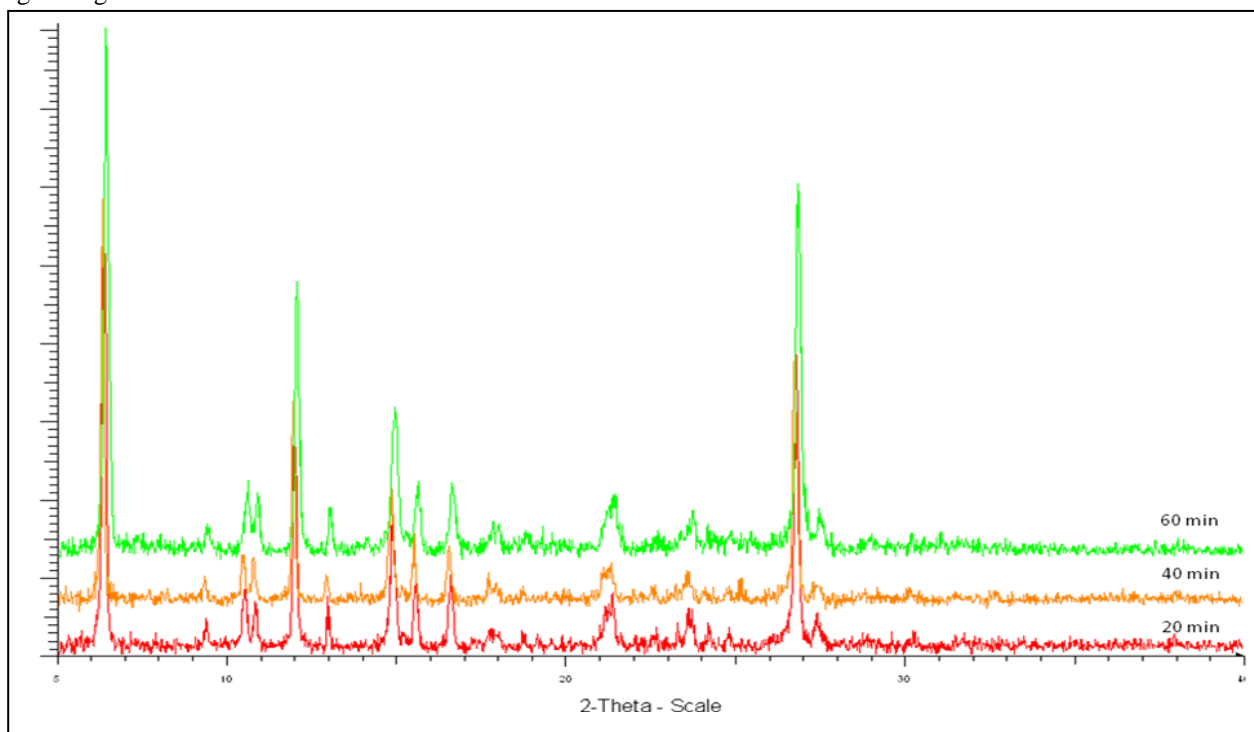
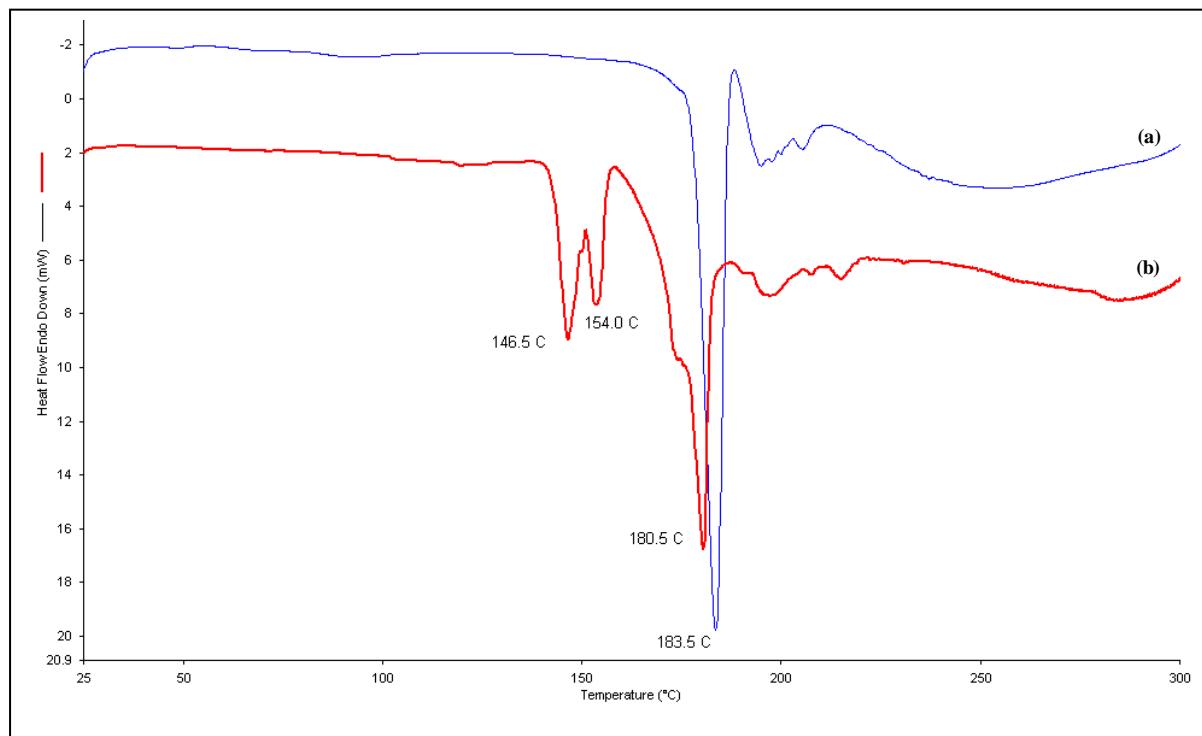
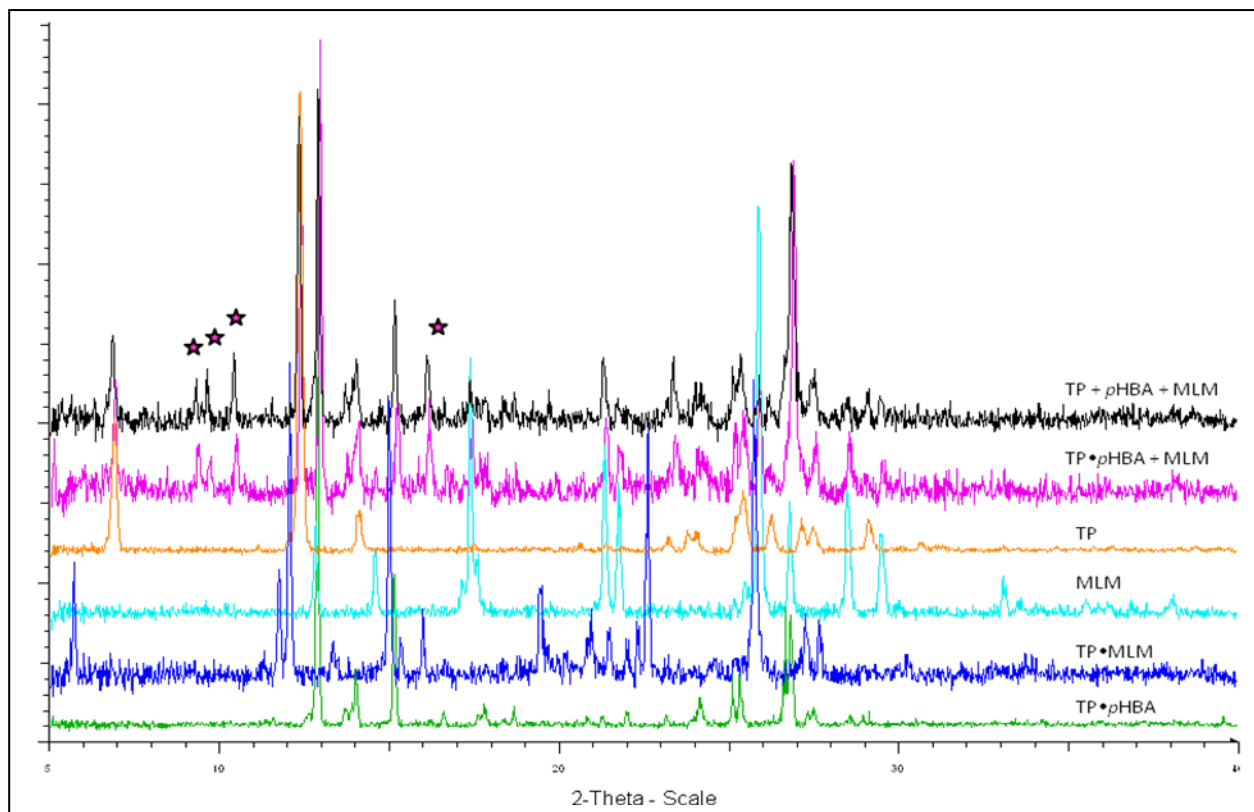


Fig.S8c- DSC heating curves comparing (a) product obtained from solution crystallization of stoichiometric amounts of TP, *p*HBA and SA to (b) a physical mixture of stoichiometric amounts of the three compounds.



S9- PXRD characterization data for experiments involving melamine (MLM)

Fig. S9a- PXRD patterns for competition and selectivity experiments involving MLM ground with EtOH.



*Peaks corresponding to $pHBA \cdot MLM$

Fig.S9b- PXRD patterns for competition experiments involving TP • pHBA and MLM ground with EtOH that examine the effect of grinding time on reaction outcome

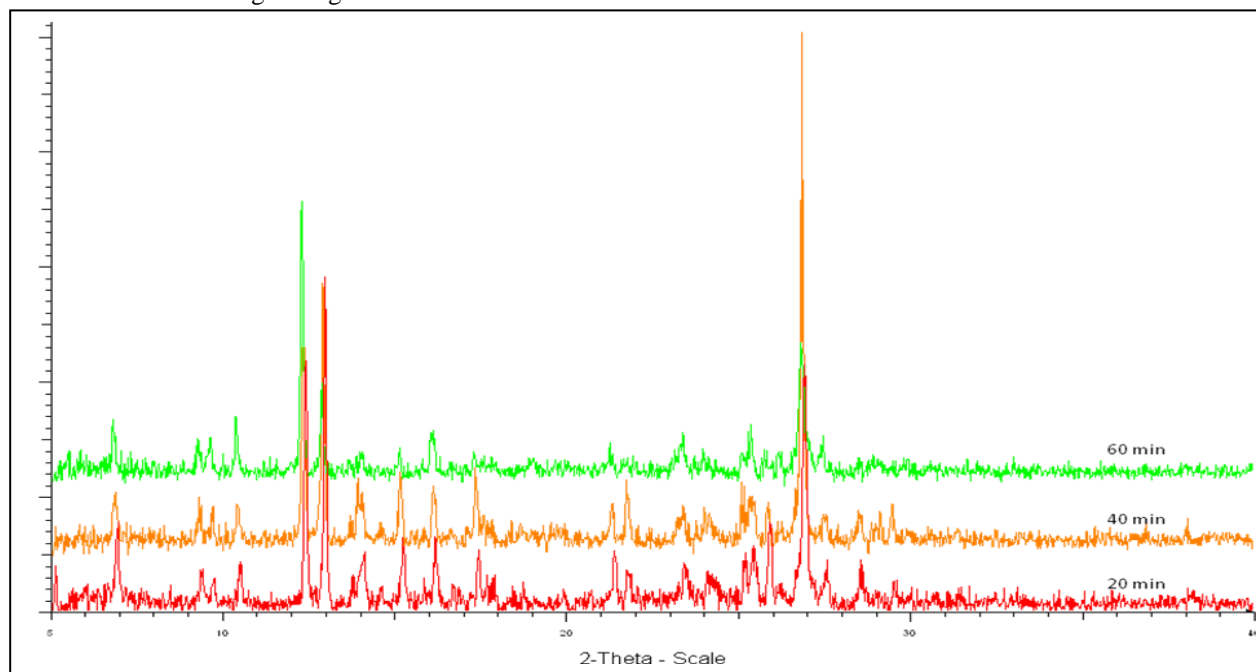


Fig. S9c- PXRD patterns from competition and selectivity experiments involving TP·pHBA and MLM that examine the effect of solvent used during SDG (solvent = EtOH or DMSO)

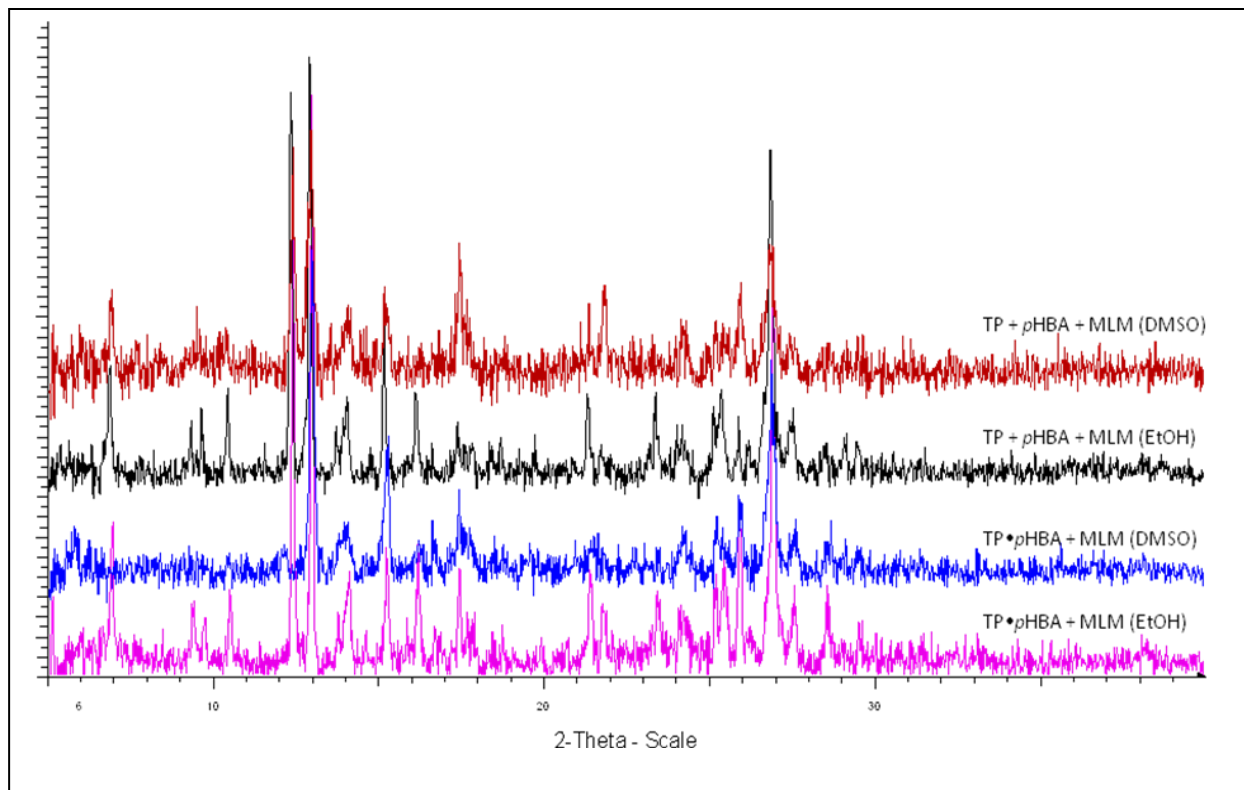
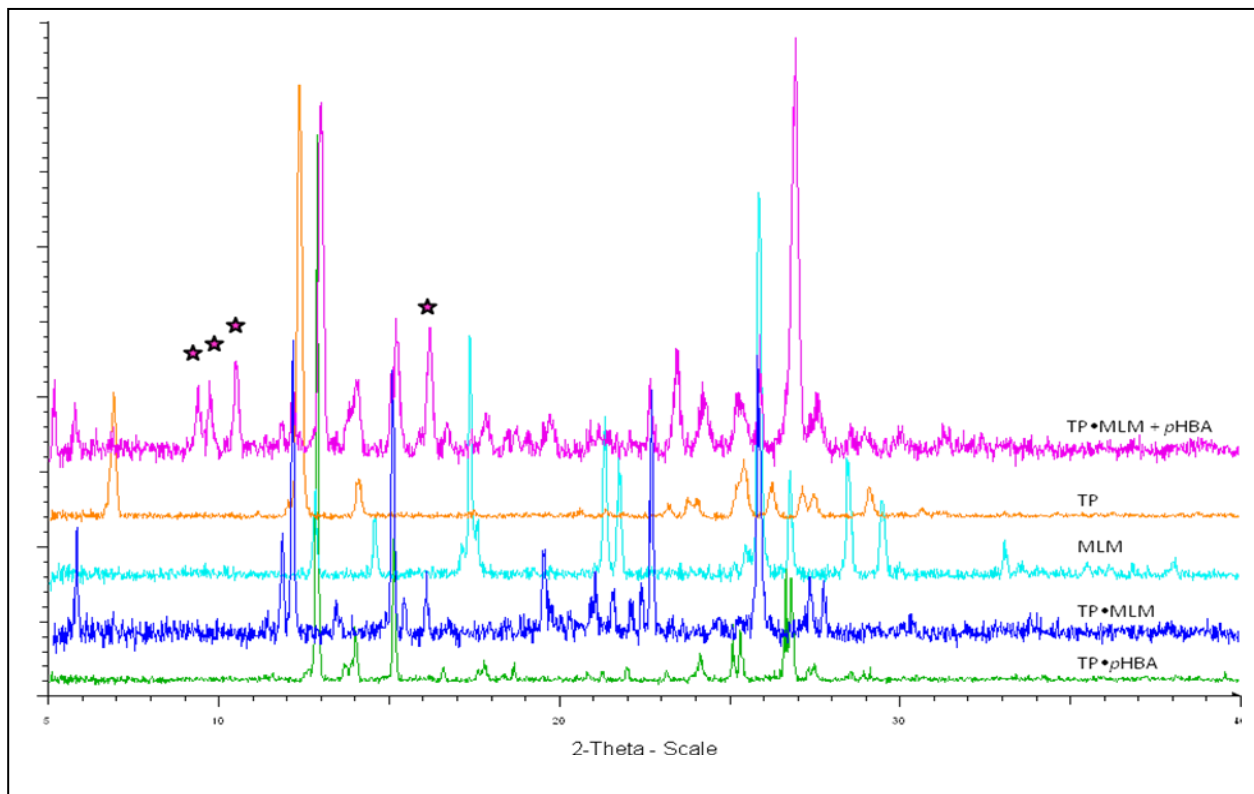
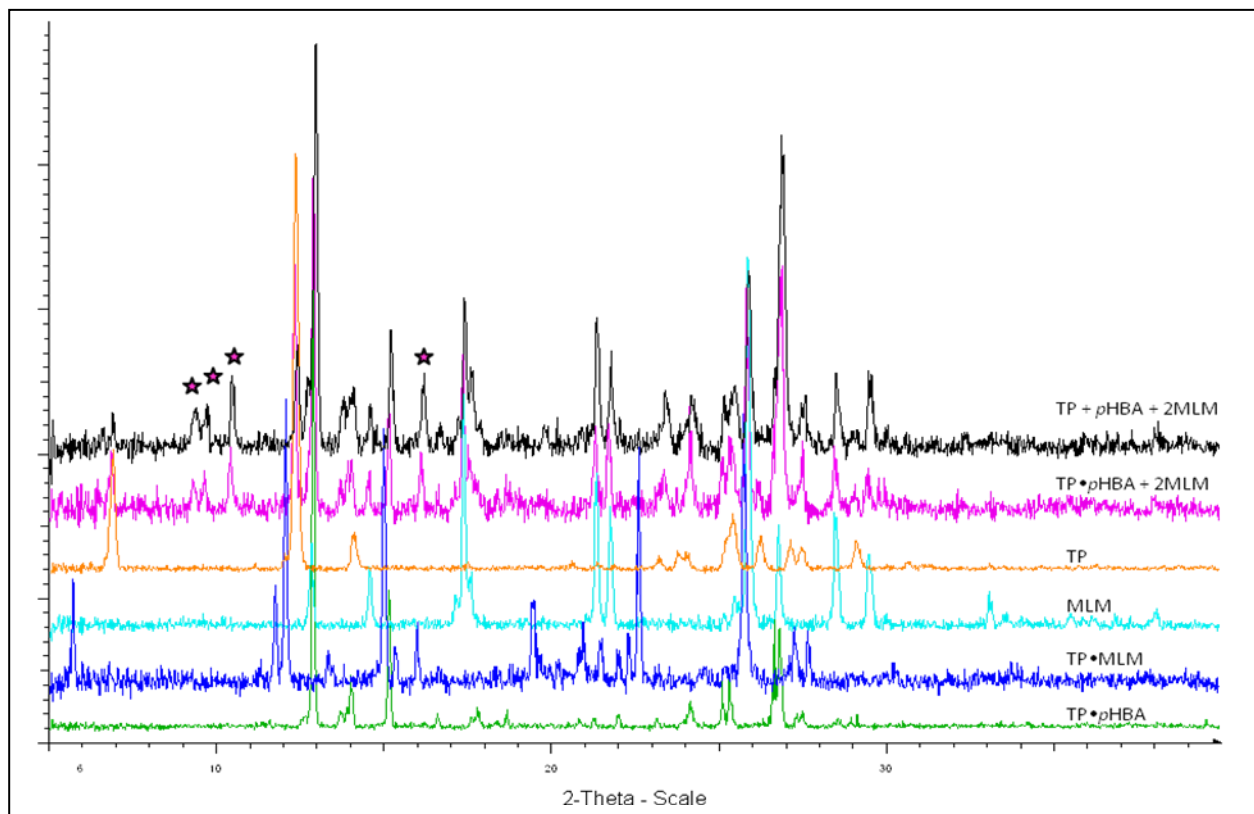


Fig.S9d- PXRD patterns for the reverse competition*Peaks correspond to pHBA•MLM



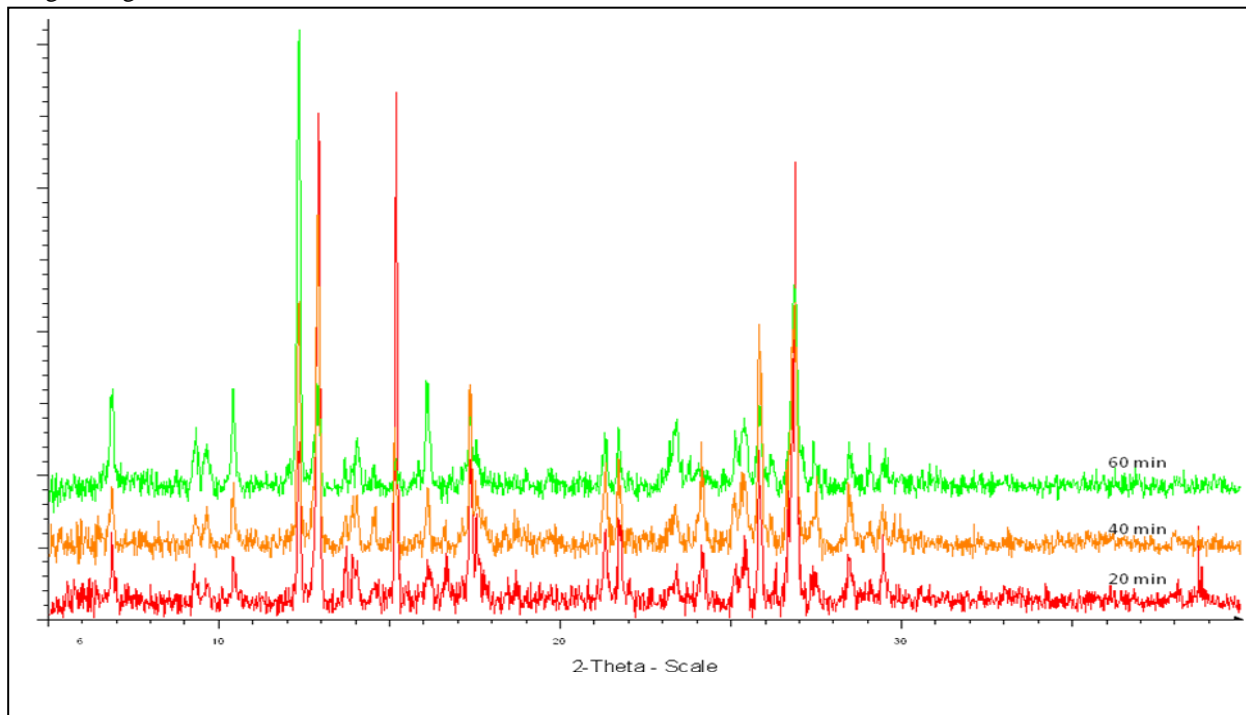
experiment involving TP•MLM and pHBA

Fig. S9e- PXRD patterns for competition and selectivity experiments involving TP•pHBA and excess MLM.



*Peaks correspond to pHBA•MLM

Fig.S9f- PXRD patterns for competition experiments involving TP•pHBA and excess MLM that examine the effect of grinding time on reaction outcome



S10- PXRD characterization data for experiments involving acetamide (ACA)

Fig. S10a- PXRD patterns for competition and selectivity experiments involving ACA.

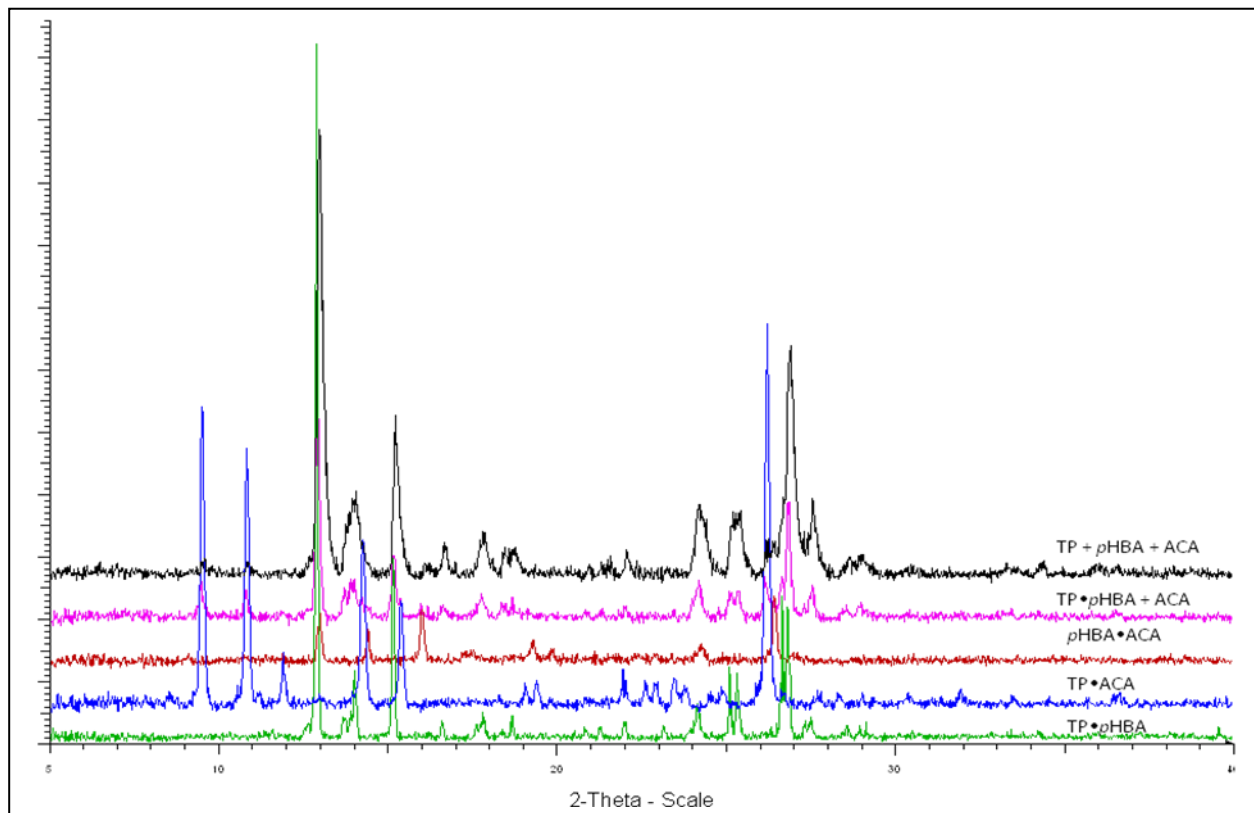


Fig.S10b- PXRD patterns for competition experiments involving TP•pHBA and ACA that examine the effect of grinding time on reaction outcome

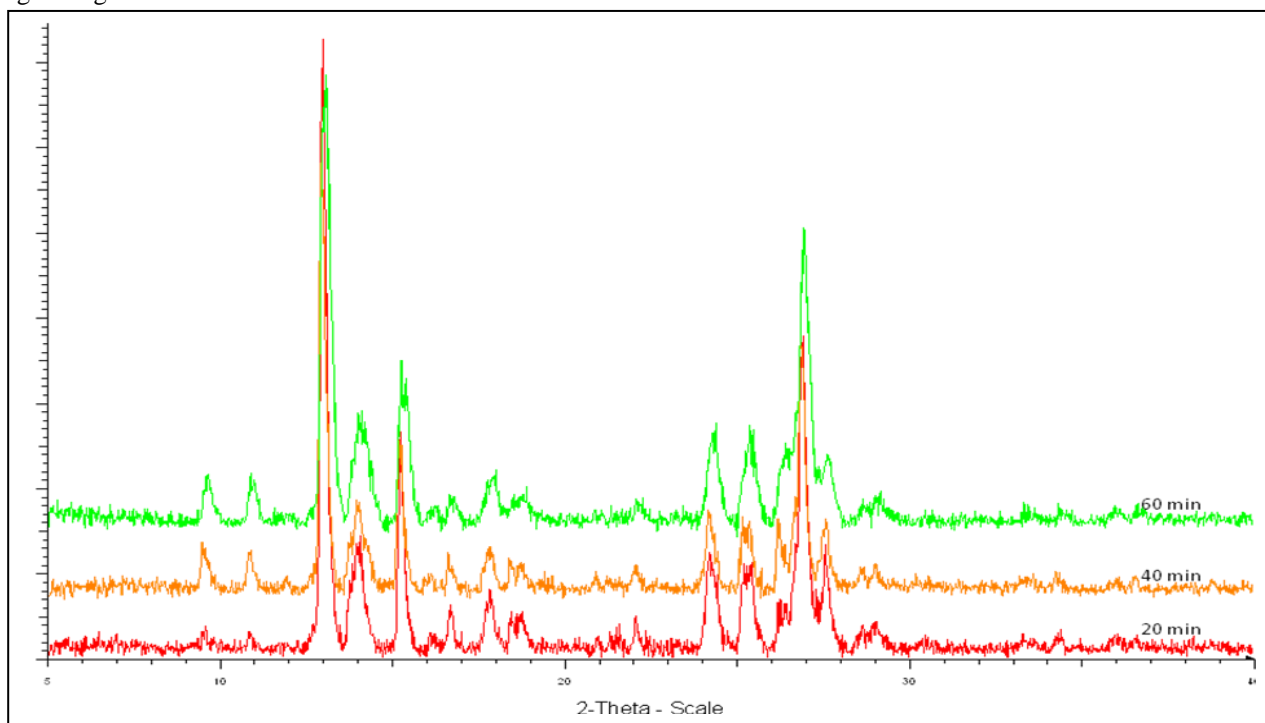


Fig. S10c- PXRD patterns for the reverse competition experiment involving stoichiometric amounts of TP•ACA and *p*HBA.

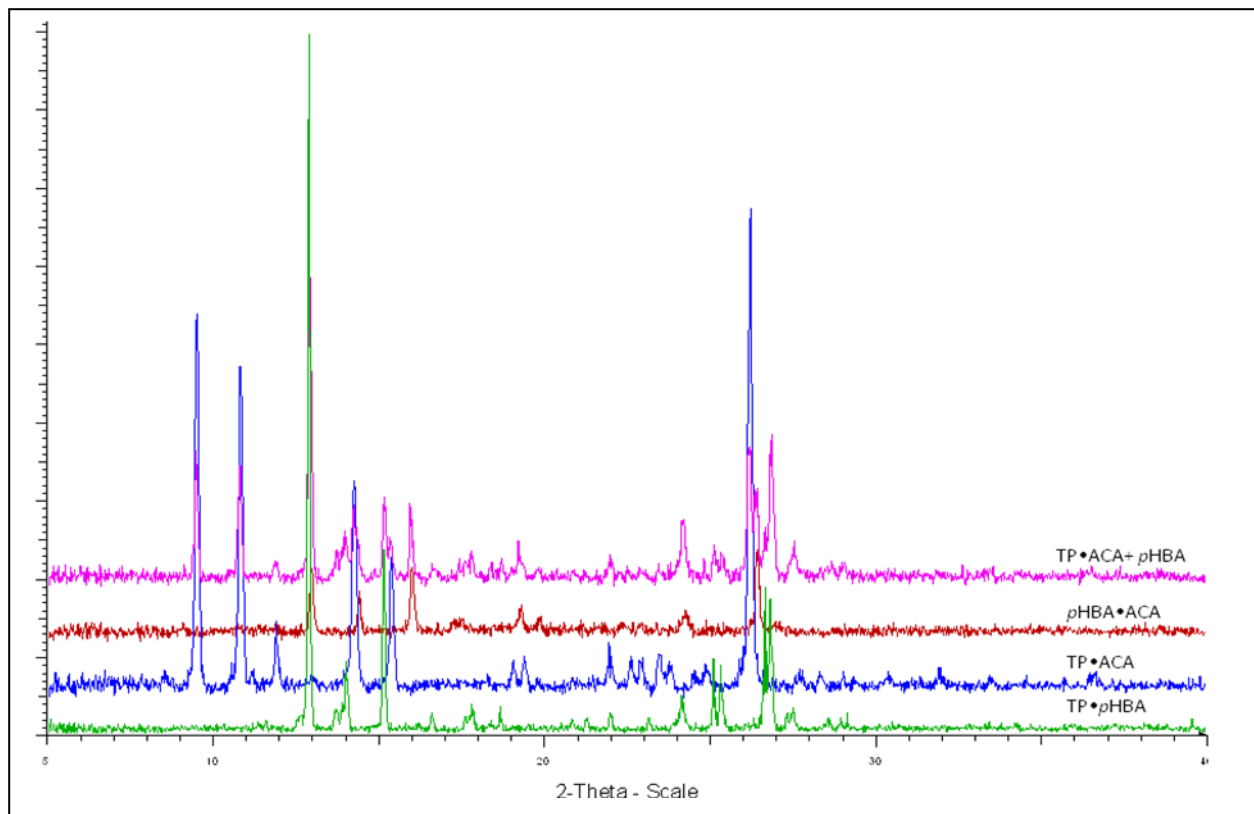


Fig.S10d-PXRD patterns for competition and selectivity experiments involving TP•*p*HBA and excess ACA

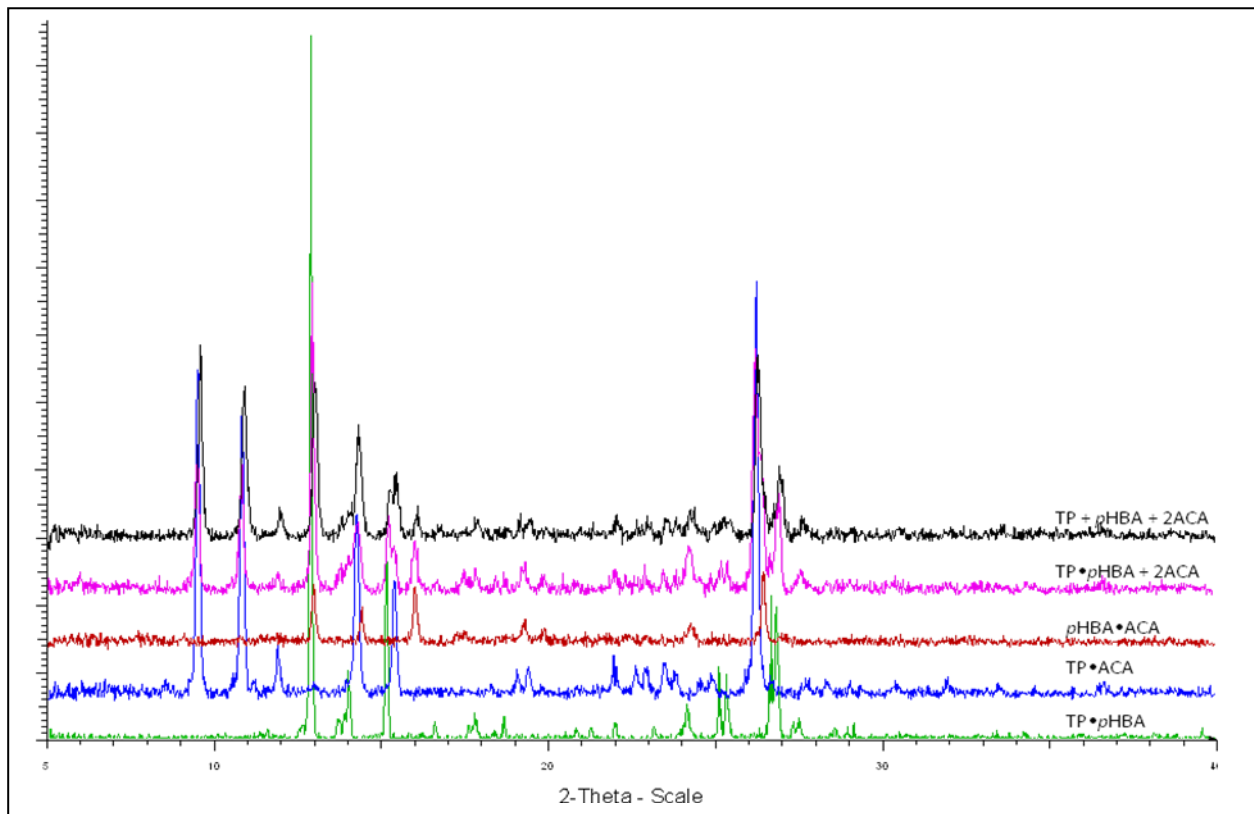
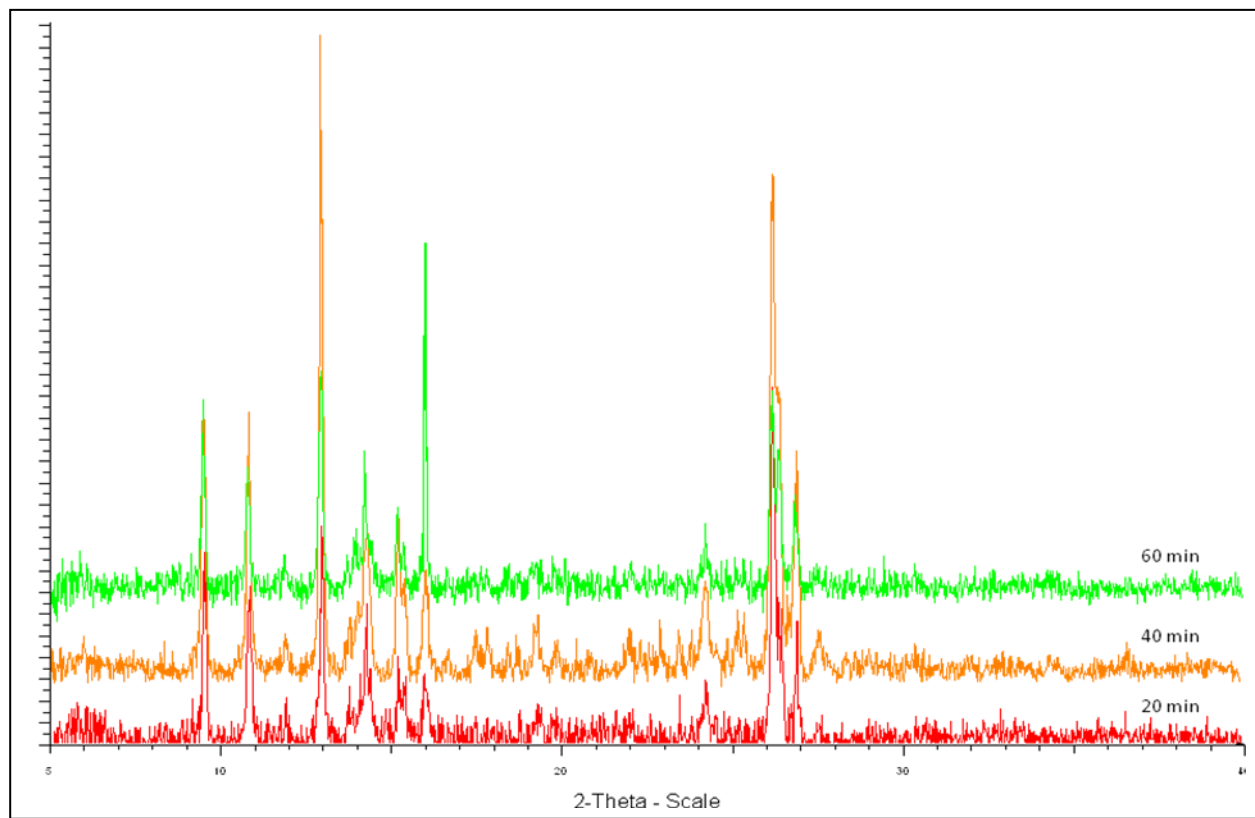


Fig. S10e- PXRD patterns for competition experiments involving TP•pHBA and excess ACA that examine the effect of grinding time on reaction outcome



S11- PXRD characterization data for experiments involving 3,5-dinitrobenzoic acid (dNBA)

Fig. S11a- PXRD patterns for competition and selectivity experiments involving dNBA.

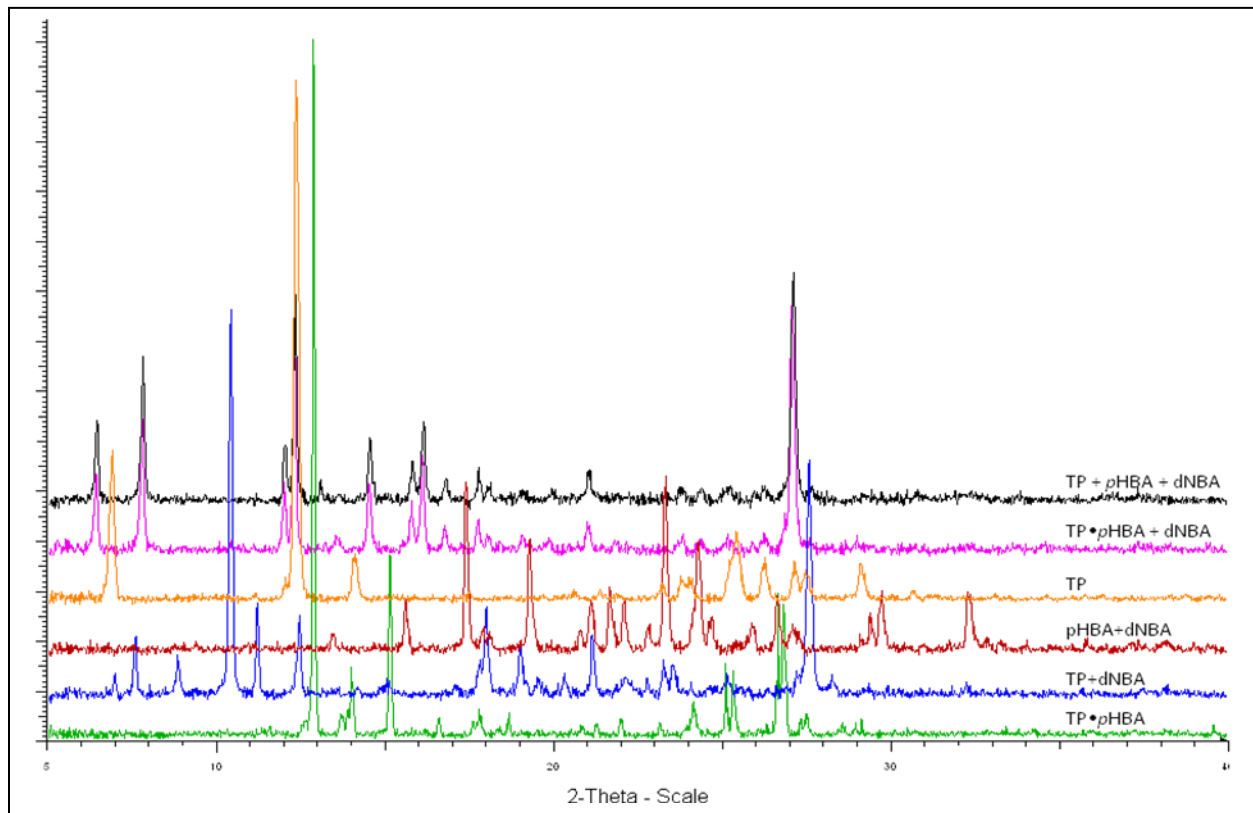


Fig.S11b- PXRD patterns for competition experiments involving TP•pHBA and dNBA that examine the effect of grinding time on reaction outcome

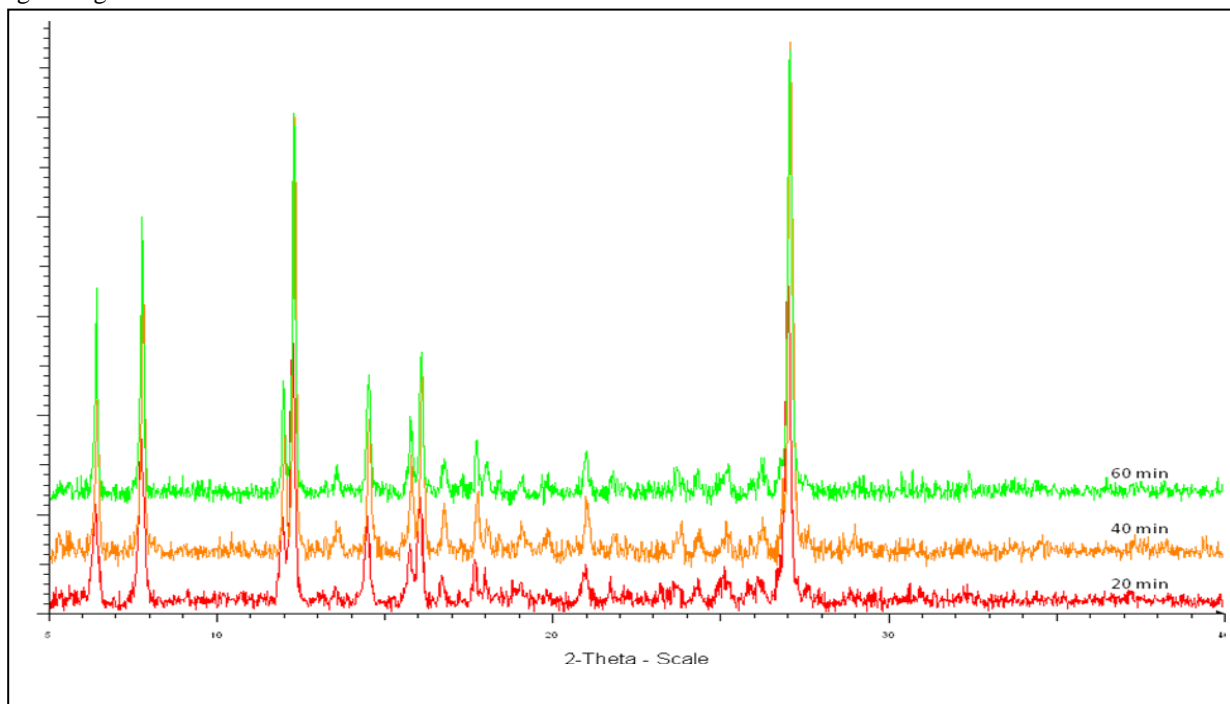
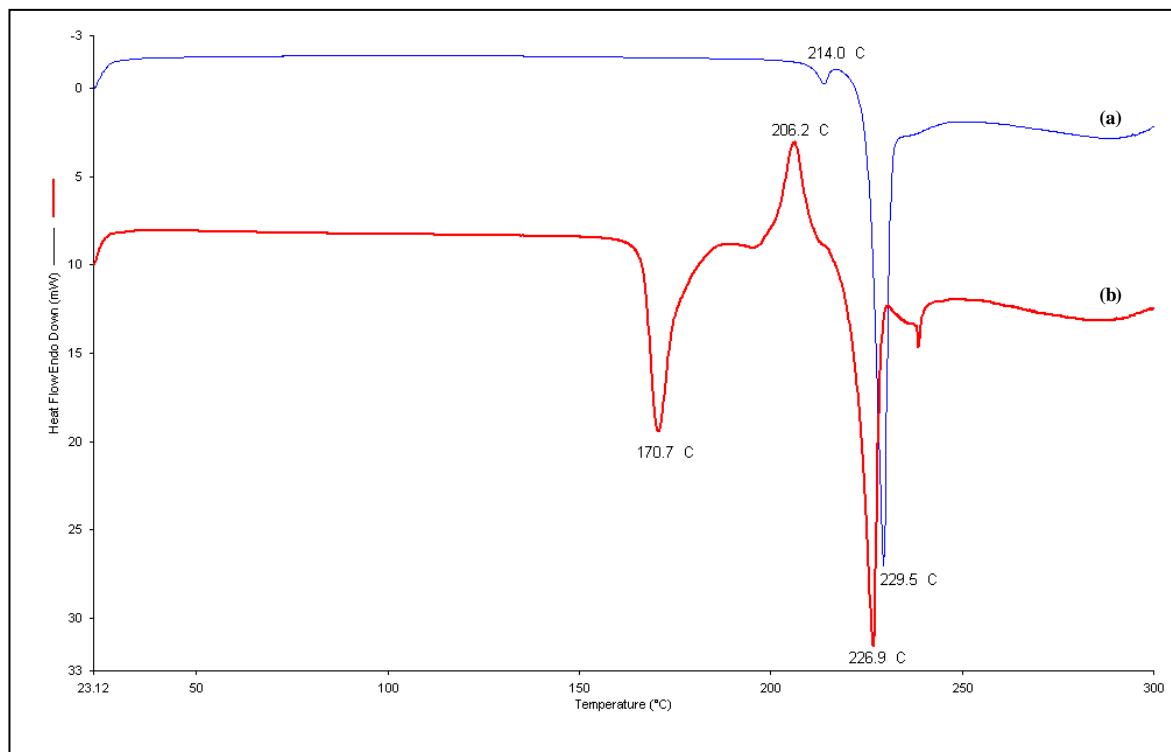
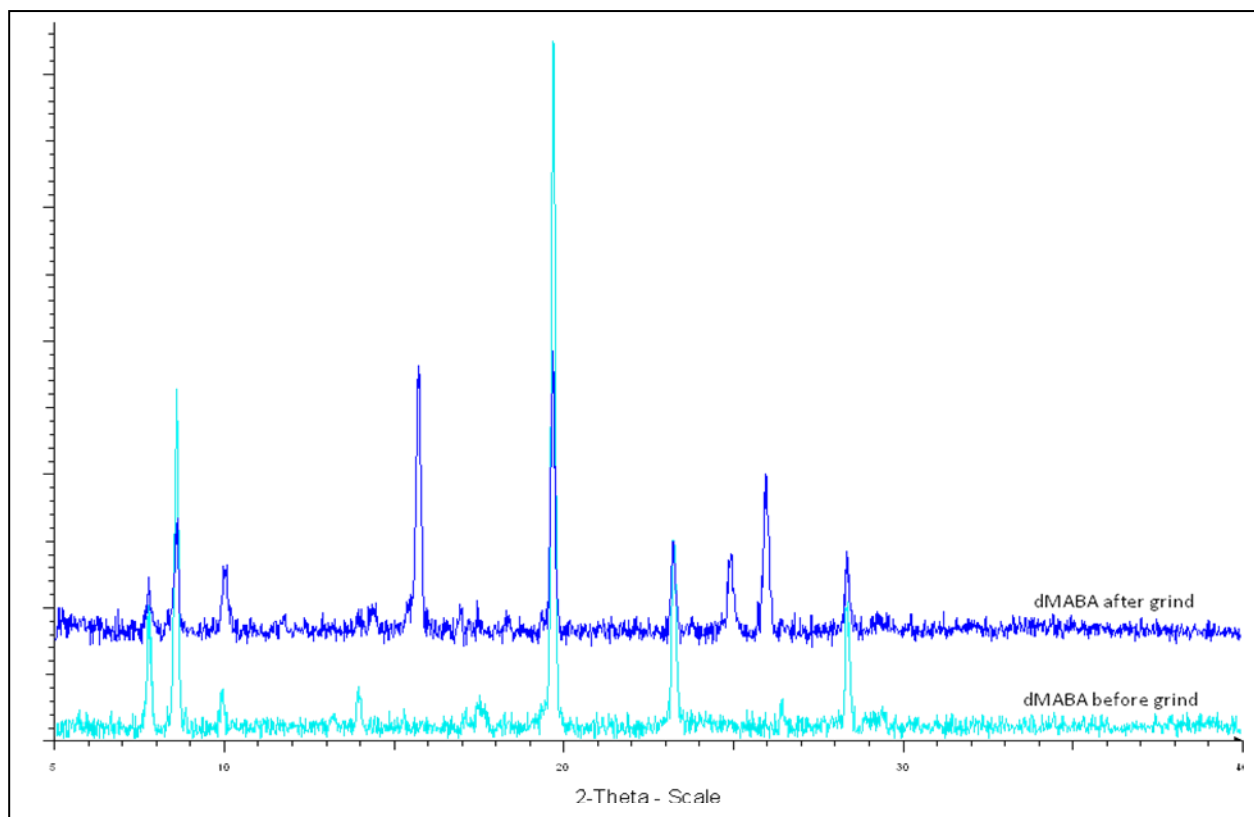


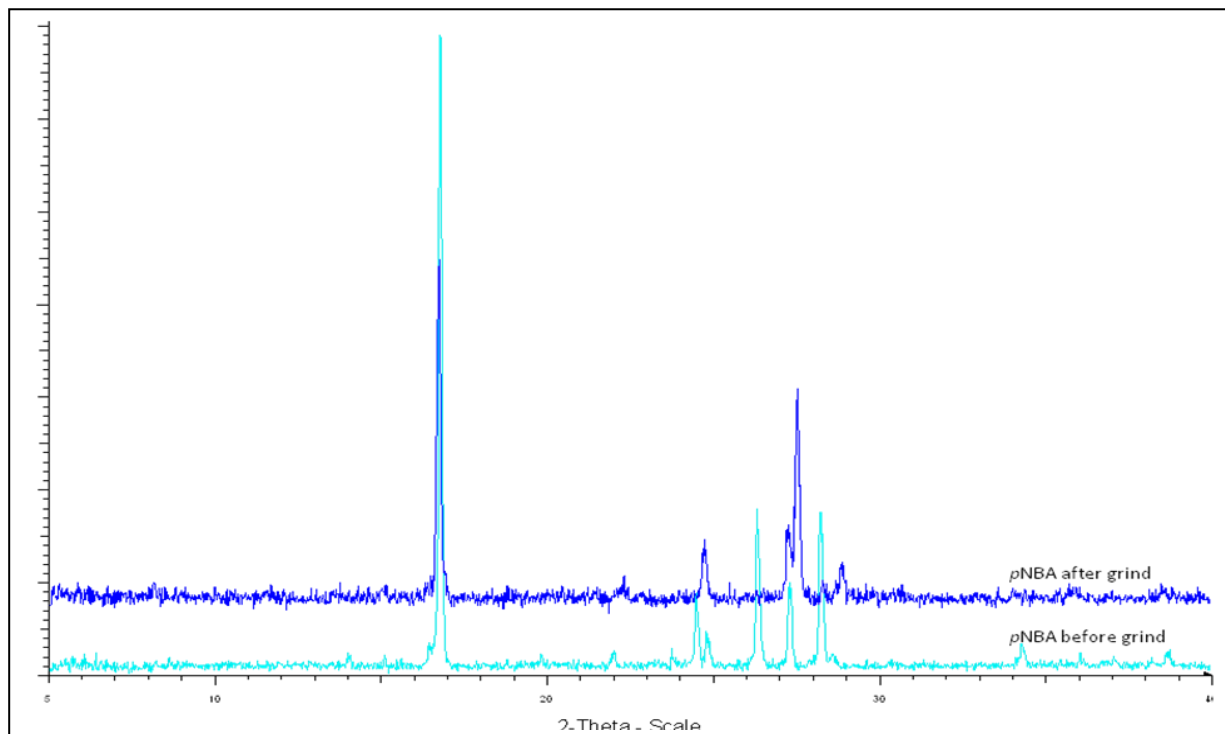
Fig.S11c- DSC heating curves comparing (a) the SDG product of TP + *p*HBA + dNBA to (b) a physical mixture of stoichiometric amounts of the three compounds.



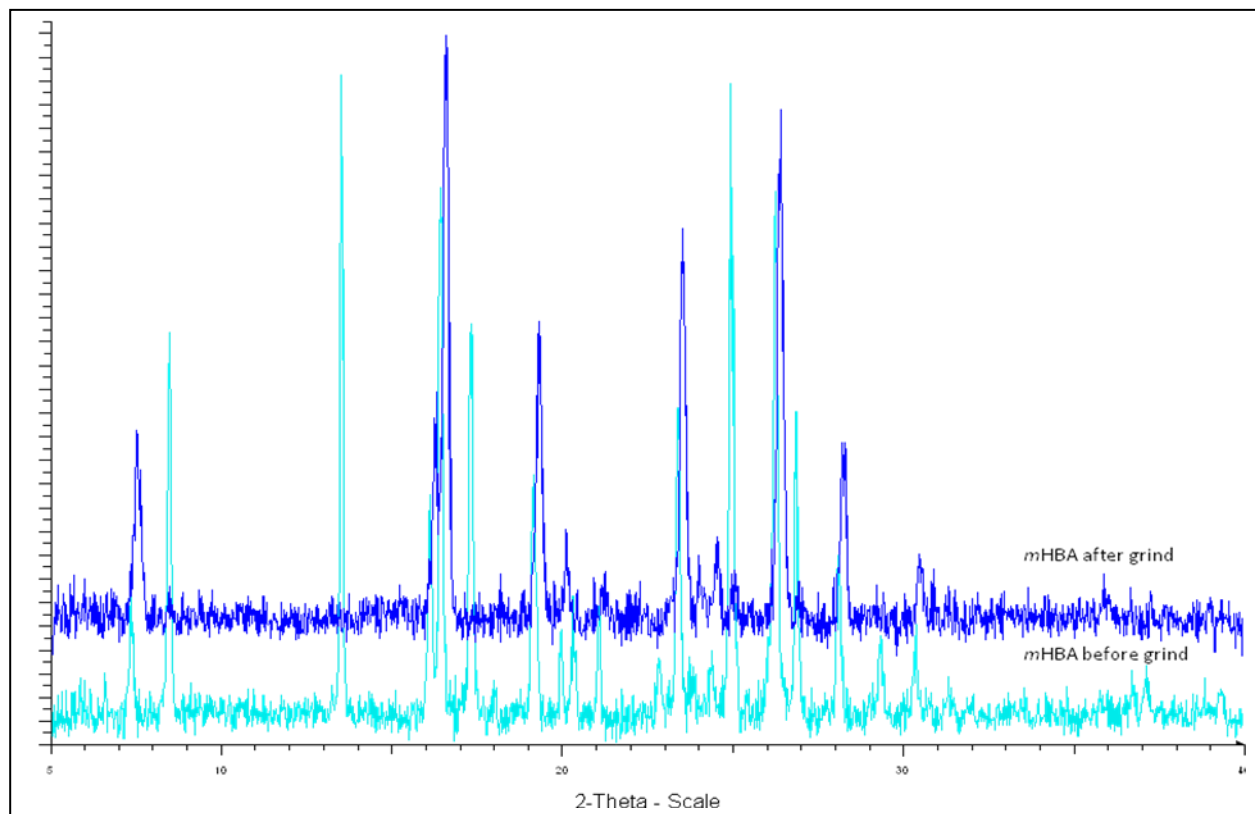
S12- PXRD patterns for dMABA before and after grinding showing a phase change



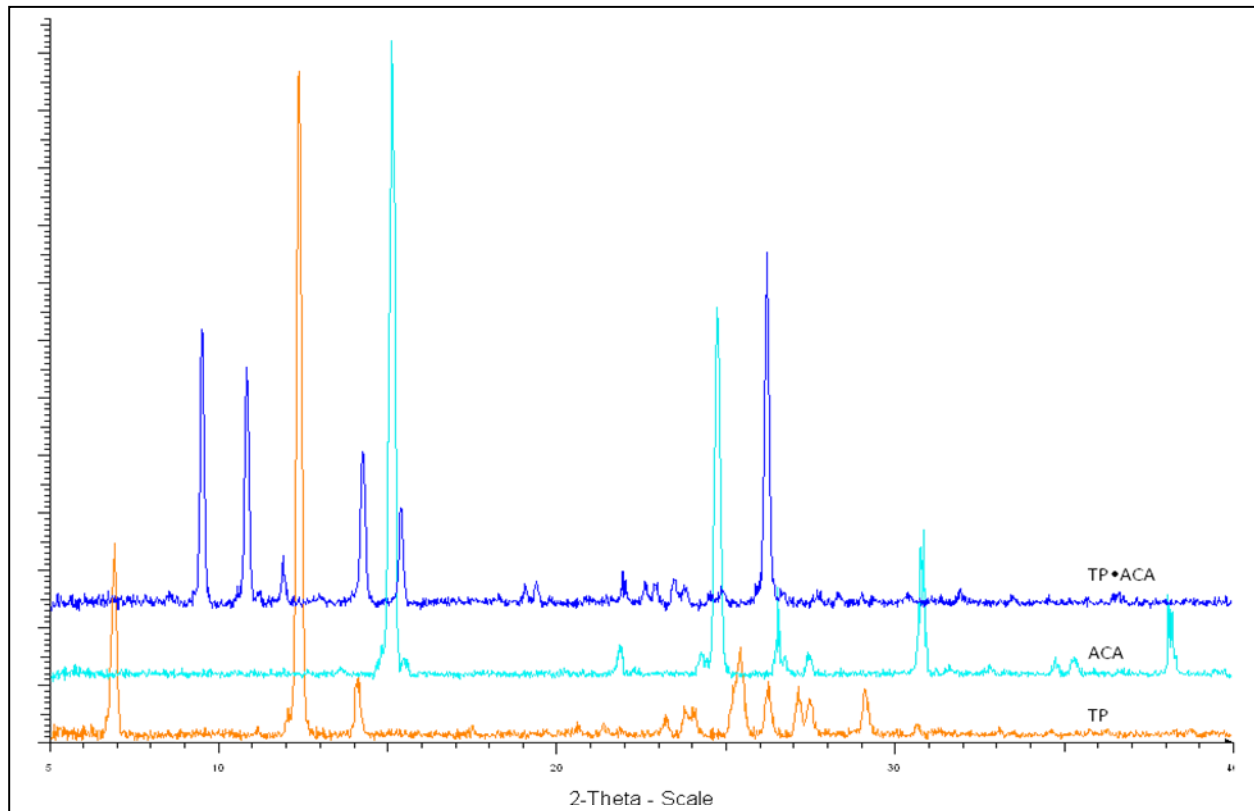
S13- PXRD patterns for pNBA before and after grinding showing a phase change



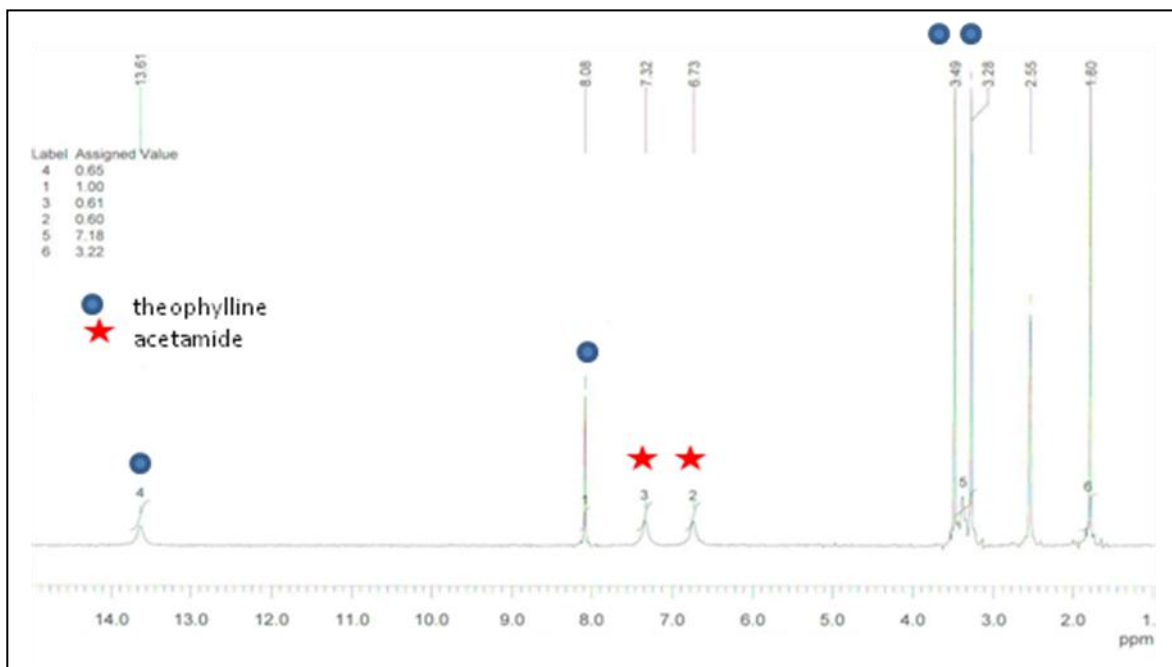
S14- PXRD patterns for *m*HBA before and after grinding showing a phase change



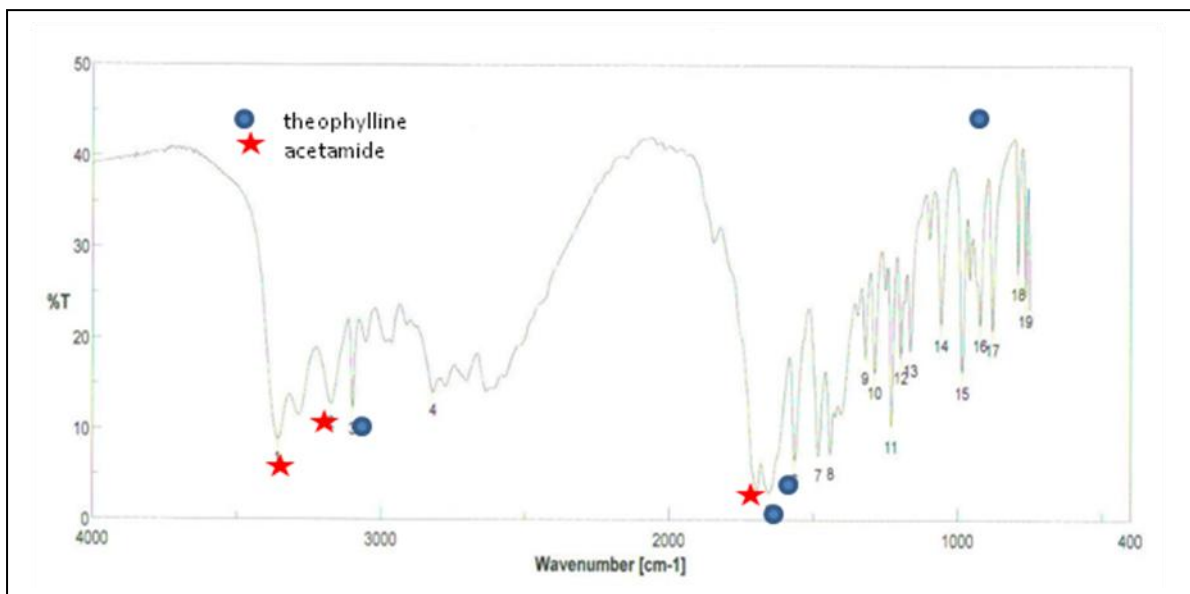
S15- PXRD pattern of TP•ACA cocrystal obtained from solution



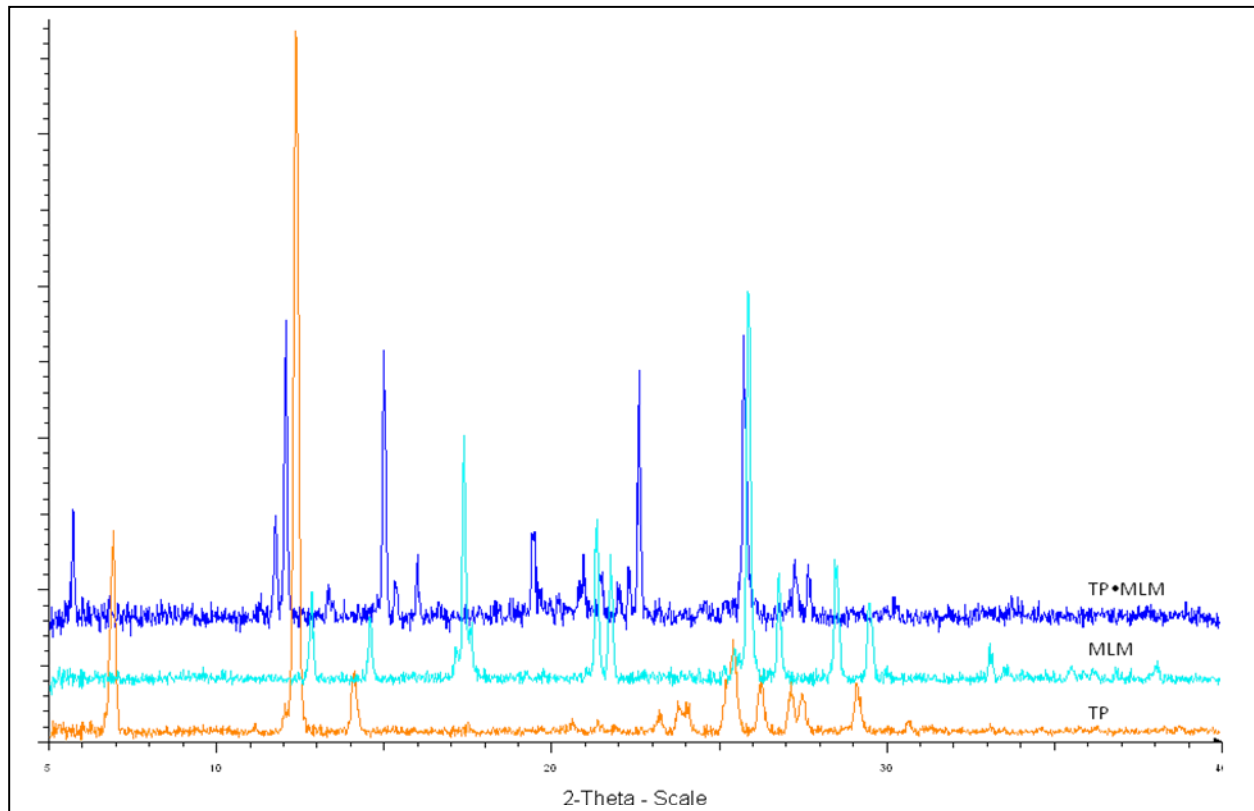
S16. ^1H NMR spectrum of TP.ACA in DMSO-d_6



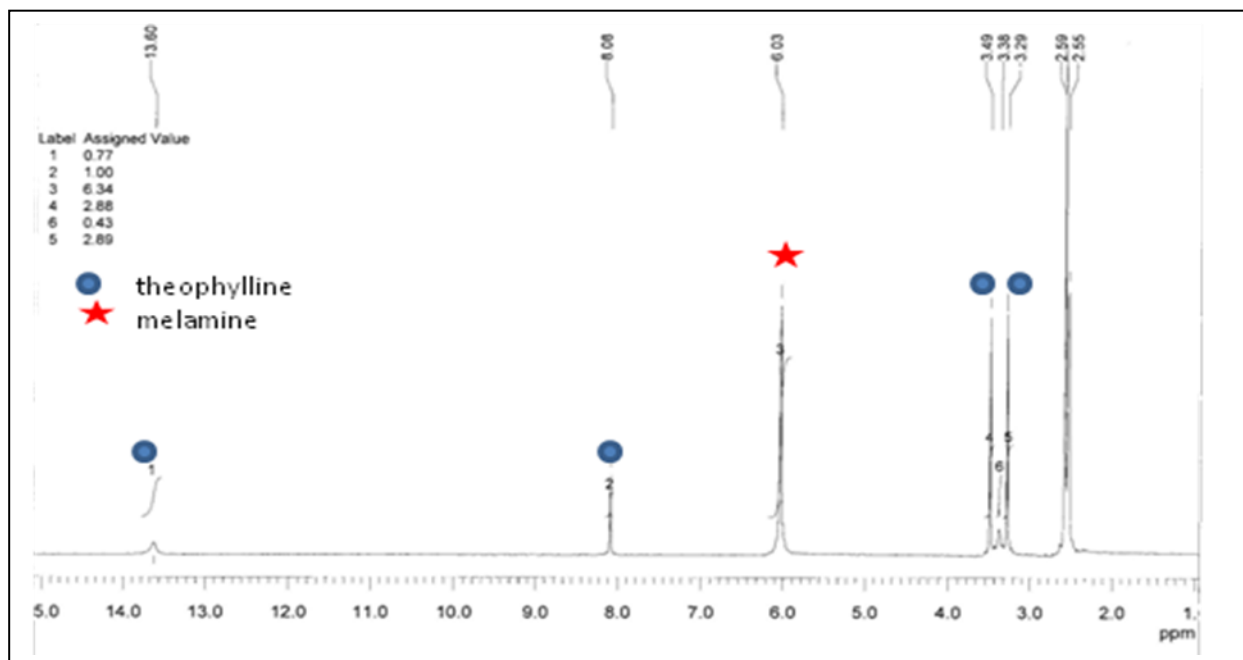
S17. IR spectrum of TP•ACA cocrystal



S18- PXRD pattern of TP•MLM cocrystal crystallized from solution



S19. ¹H NMR spectrum of TP•MLM in DMSO-d₆



S20. Crystal data and structure refinement for TP•MLM•DMSO.

Empirical formula	C ₁₂ H ₂₀ N ₁₀ O ₃ S	
Formula weight	384.44	
Temperature	293(2) K	
Wavelength	0.71073 Å	
Crystal system	Monoclinic	
Space group	P21/c	
Unit cell dimensions	a = 15.4964(11) Å	α = 90°.
	b = 8.8674(6) Å	β = 109.4230(10)°.
	c = 13.2985(9) Å	γ = 90°.
Volume	1723.4(2) Å ³	
Z	4	
Density (calculated)	1.482 Mg/m ³	
Absorption coefficient	0.227 mm ⁻¹	
F(000)	808	
Crystal size	0.2 x 0.2 x 0.2 mm ³	
Theta range for data collection	2.69 to 28.58°.	
Index ranges	-19 ≤ h ≤ 20, -11 ≤ k ≤ 11, -17 ≤ l ≤ 17	
Reflections collected	19732	
Independent reflections	4187 [R(int) = 0.0293]	
Completeness to theta = 25.00°	100.0 %	
Refinement method	Full-matrix least-squares on F ²	
Data / restraints / parameters	4187 / 0 / 271	
Goodness-of-fit on F ²	1.044	
Final R indices [I > 2σ(I)]	R1 = 0.0345, wR2 = 0.0852	
R indices (all data)	R1 = 0.0443, wR2 = 0.0913	
Largest diff. peak and hole	0.334 and -0.332 e.Å ⁻³	

S21. Table of hydrogen bonds for TP•MLM•DMSO [\AA and $^\circ$].

D-H...A	d(D-H)	d(H...A)	d(D...A)	$\angle(\text{DHA})$
N(8)-H(2)...O(1)#1	0.881(18)	2.010(19)	2.8781(16)	168.4(16)
N(10)-H(3)...O(2)#2	0.878(19)	2.209(19)	3.0495(16)	160.1(17)
N(8)-H(1)...N(4)#3	0.87(2)	2.13(2)	2.9887(17)	171.4(16)
N(10)-H(4)...O(3)#4	0.89(2)	2.11(2)	2.9893(16)	167.7(17)
N(1)-H(10)...N(7)#3	0.94(2)	1.86(2)	2.7995(16)	176.0(19)
N(9)-H(12)...O(3)#5	0.86(2)	2.145(19)	2.8145(16)	134.4(17)
N(9)-H(11)...N(6)#6	0.91(2)	2.12(2)	3.0317(17)	176.4(18)

Symmetry transformations used to generate equivalent atoms:

#1 $-x+1, y-1/2, -z+3/2$ #2 $x, -y-3/2, z-1/2$ #3 $-x+1, y+1/2, -z+3/2$

#4 $-x, y-1/2, -z+1/2$ #5 $x, -y-1/2, z+1/2$ #6 $-x, -y-1, -z+1$

S22. Crystal structure of TP•MLM•DMSO

